Asymptotic analysis of multi-phase-field models: A thorough consideration of junctions

E. S. Nani[*]
Institute of Applied Materials (IAM-CMS), Karlsruhe Institute of Technology (KIT), Geb. 30.48, Strasse am Forum 7, 76131 Karlsruhe, Germany

Britta Nestler[†]
Institute of Applied Materials (IAM-CMS), Karlsruhe Institute of Technology (KIT), Geb. 30.48, Strasse am Forum 7, 76131 Karlsruhe, Germany
and Institute of Digital Materials Science (IDM), Karlsruhe University of Applied Sciences, Moltkestrasse 30, 76133 Karlsruhe, Germany

(Received 27 January 2022; accepted 11 January 2023; published 27 February 2023)

The solutions of multi-phase-field models exhibit boundary layer behavior not only along the binary interfaces but also at the common contacts of three or more phases, i.e., junctions. Hence, to completely determine the asymptotic behavior of a multi-phase-field model, the inner analysis of both types of layers has to be carried out, whereas, traditionally, the junctions part is ignored. This is remedied in the current work for a phase-field model of simple grain growth in two spatial dimensions. Since the junction neighbourhoods are fundamentally different from those of the binary interfaces, pertinent matching conditions had to be derived from scratch, which is also accomplished in a detailed manner. The leading-order matching analysis of the junctions exposed the restrictions present on the interfacial arrangement at the common meeting point, while the next-to-the-leading one uncovered the law governing the instantaneous motion of the latter. In particular, it is predicted for the considered model that the Young's law is always satisfied at a triple point, whether or not it is at rest. Surprisingly, the mobilities and the curvatures of the involving interfaces as well as the driving forces on the them do not affect this result. However, they do play a significant role in determining the instantaneous velocity of the junction point. The study has opened up many new directions for future research.

DOI: 10.1103/PhysRevE.107.024803

I. INTRODUCTION

Phase-field methodology is fast becoming ubiquitous in the modeling of evolution in heterogeneous media [1–21]. The unique benefits which it offers earn this approach the preference it receives over the sharp-interface treatments. However, due to the broad, or sometimes even rough, nature of the arguments invoked in composing the phase-field modeling equations, additional analysis is warranted to demonstrate the correspondence with the right free-boundary problem. Asymptotic analysis is a tool which helps establish this connection.

A number of scalar phase-field models have been proposed to handle diverse phenomena like spinodal decomposition [22,23], dendritic solidification [24–26], bulk and/or surface diffusion mediated Ostwald ripening [27,28], etc. The asymptotic analyses of these models have also been carried out demonstrating a successful capture of the right physics in each case [29–33]. The predictions of the perturbative analyses are in turn verified numerically through interface width reduction studies or by comparing against the sharp-interface solutions for appropriate benchmark cases [34]. Thus, the phase-field program can be safely claimed to have been executed to a fair level of completion in the scalar case.

The situation, however, is not so plain in the case of multi-phase evolutions: Front-tracking becomes too formidable to obtain sharp-interface solutions for any of the representative benchmark cases. The vector phase-indicator evolution equations are seldom studied in a rigorous manner through asymptotic methods. And even before any of these, the free-boundary problems themselves cannot be completely and unobjectionably written down, as the sharp-interface governing laws for multiple-phase contacts are not fully known, or are under debate most of the time.

The disagreement about the existence of a separate Young's type law for dynamical situations is an instance of the latter. Young's law proposes how three interfaces at rest should arrange themselves relative to each other at their common meeting manifold depending on their excess energies [35]. This has well been verified experimentally, at least in the case of fluid membranes or surfaces of gas bubbles. However, whether the law continues to hold even for a moving tri-junction, i.e., when the system is evolving, is still unsettled. The scientific community hasn't been able to come to a common consensus about the conclusion, with some arguing that it does and others favoring the existence of a separate dynamical Young's law for junctions in motion. No real experimental data seems to exist favoring either side of the debate, definitely not for interfaces between condensed phases.

[*]sumanth.enugala@kit.edu
[†]britta.nestler@kit.edu

Given this state of affairs, it is vital to know with certainty, at least, what the phase-field side of the picture is, i.e., what the phase-field models recover. Ideally, one would want to have models capable of capturing each and every possibility, so that they can be appropriately deployed depending on the demands of the problem at hand. Indeed, many models have been constructed which have been demonstrated to recover the Young's law for both the static and the dynamic situations [36,37], and some which break it in the latter case. In yet other implementations, instead of the actual speed of the junction, the mobilities of the involving interfaces are seen to have an effect on the recovered trijunctions angles [38–40]. However, all these demonstrations are through numerical integrations of the phase-field equations and subsequent analysis of the simulated microstructures. Whereas, a stronger justification would be through analytical methods, thus signifying the elevated importance of asymptotic analysis for multi-phase-field models. However, such an analysis has never been carried out in a full-fledged and rigorous manner bar two exceptions [41,42].

The multi-phase-field evolution equations have always been reduced to two-phase models (which essentially reduce further to scalar phase-field equations due to the oft-employed summation constraint) using heuristic arguments before analyzing through asymptotic methods. Since junctions cannot be handled in such a simplification, they are completely left out of the analysis. The first exception, and practically the complete solution, is due to Bronsard and Reitich [41] who performed a rigorous handling of the multi-phase equations of simple three-grain evolution. This was later adopted by Wheeler *et al.* [42] for the problem of eutectic solidification. In Ref. [43], the current authors have extended Bronsard and Reitich's treatment to a grain growth model for any number of phases and various timescales. However, the consideration is only limited to the study of binary interfaces. In the current article, the junctions part of the extension will be presented. While Bronsard and Reitich stopped after performing the leading-order matching analysis of the junctions, the next-to-the-leading order is also studied in the current article.

The content-wise breakdown of the rest of the paper is as follows: Section II recalls the phase-field model of simple grain growth studied in Ref. [43] and sets the stage for the local analysis of junctions before working out the details. As in Ref. [43], only two spatial dimensions will be concerned for the entire study. An important ingredient of the asymptotic procedure is the exploitation of the matching conditions; Sec. III along with Appendix A is dedicated to their detailed derivation. The subtle aspects of the analysis are given special attention in the discussion provided in Sec. IV. Finally, some concluding remarks are presented in Sec. V.

II. ASYMPTOTIC ANALYSIS OF MULTI-PHASE-FIELD MODEL OF GRAIN GROWTH

Multi-phase-field models are employed to study evolution in systems featuring at least three distinct homogeneous bulks. The basic idea behind their construction is a plain extension of the philosophy of the scalar models: Each stable phase is assigned a distinct value, and the energy associated with it is chosen at a minimum, while the intermediate values are penalized so that they remain restricted to thin interfacial zones. The sustenance of the diffuseness of the interfaces is ensured by the usage of gradient energy terms. Since more than two distinct values have to correspond to the equilibrium phases, there is no choice but to increase the dimensionality of the phase-indicator [44]. This in turn requires the introduction of multidimensional wells as counterparts to double-wells for the penalization of the intermediate phases [43]. For convenience, the standard basis vector values are chosen to be the ones corresponding to the stable phases.

As the aim of the current study is to demonstrate the procedure of performing the asymptotics for multi-phase-field models, we try to tone down the complexity as much as possbile. Hence, we do not consider any transport fields, and just work with phase-indicator evolution. Furthermore, the gradient energy terms are also chosen in the simplest manner possible, i.e., with same weights irrespective of the component of the vector phase-indicator. Such a simplest multi-phase-field model has been previously leveraged heavily for simulating the grain growth phenomenon in polycrystalline single phase materials. In this context, the interpretation is that each equilibrium value of the vector phase-field variable marks a distinct grain orientation present in the initial microstructure. Thus, the free-energy functional is as follows:

$$F = \int \left(f_\alpha g_\alpha(\phi) + \frac{1}{\epsilon}\gamma W(\phi) + \epsilon \frac{\gamma}{2} |\nabla \phi|^2 \right) dV, \quad (1)$$

where ϕ is the vector-valued phase-field variable with N components, i.e., $\phi = (\phi_1, \phi_2, \ldots, \phi_N)$, where each component characterizes a distinct orientation (please refer to Ref. [43] for elaboration). $W(\phi)$ is the dimensionless multi-well potential. f_α is the bulk energy specifier of the αth orientation. $g_\alpha(\phi)$ is the interpolation function conjugate to the αth orientation, i.e., it satisfies $g_\alpha(\phi) = 1$ when $\phi_\alpha = 1$, $g_\alpha(\phi) = 0$ when $\phi_\alpha = 0$, and $\frac{\partial g_\alpha(\phi)}{\partial \phi_\alpha} = 0$ when $\phi_\alpha = 0$ or 1. γ is a prefactor carrying the units of interfacial energy. Finally, ϵ is the interface width, or more precisely, "the extent of spread of the inter-phase region" parameter. We clarify that the dimensionality N of the phase-indicator is the number of different grain orientations present in the starting configuration, and not necessarily the total number of grains themselves, as repetitions are allowed. That is, a number of grains with same oreintation can be smeared all across the micrograph, and they will all be assigned the same ϕ value.

The governing equation for multigrain evolution can be derived from Eq. (1) in a straightforward manner by demanding monotonic reduction of free-energy. It takes the following form:

$$\tau(\phi)\frac{\partial \phi_\beta}{\partial t} = -\frac{1}{\epsilon} f_\alpha \frac{\partial g_\alpha(\phi)}{\partial \phi_\beta} - \frac{1}{\epsilon^2}\gamma \frac{\partial W(\phi)}{\partial \phi_\beta} + \gamma \nabla^2 \phi_\beta - \lambda,$$
$$\beta \in \{1, 2, \cdots, N\}, \quad (2)$$

where λ is the Lagrange multiplier which ensures the summation constraint, $\sum_{\alpha=1}^{N} \phi_\alpha = 1$, when the initial filling also satisfies it. Its expansion is $\lambda = \frac{1}{N}\sum_{\beta=1}^{N} -\frac{\delta F}{\delta \phi_\beta}$, with $-\frac{\delta F}{\delta \phi_\beta}$ standing for the right-hand side (r.h.s.) of Eq. (2) excluding λ. $\tau(\phi)$ is the inverse mobilities interpolating function.

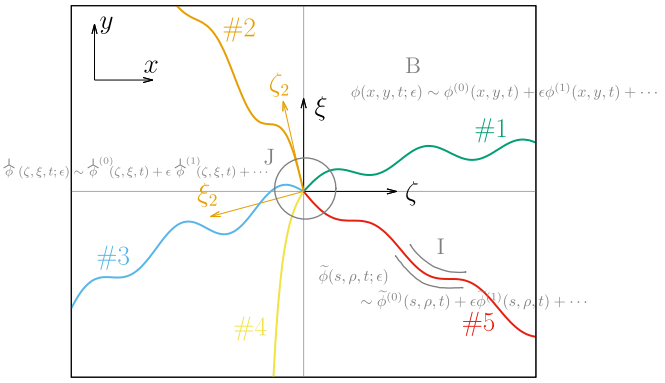

FIG. 1. Five interfaces meeting to form a junction. The junction neighborhood, a small strip around a binary interface and a subregion within one of the bulks are highlighted. x-y is the laboratory coordinate frame corresponding to the outer coordinates and ζ-ξ is the local frame. The interfaces are numbered with reference to the ζ axis by starting there and moving in the counter clockwise direction. The local coordinate system rotated so as to align the ζ axis with the tangent of an interface and suffixed with the number assigned to the latter is also shown exemplarily for the second interface (i.e., interface #2).

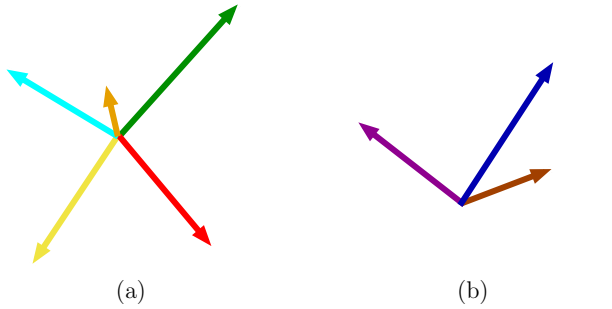

FIG. 2. Some example ray-diagram constructions. Panel (a) corresponds to the interfacial configuration of Fig. 1, while panel (b) gives an instance of a ray diagram of a special kind (please refer to the main text).

Strictly speaking, the only kind of problems for which the above model accurately applies to is that of evolution of bubbles in a soap froth. This is because some of the anisotropy effects that actually exist between grains in polycrystalline microstructures are neglected in the current treatment. Of course, by choosing the multiwell $W(\phi)$ in an appropriately asymmetric fashion, distinct pairs of grain orientations possessing surface tensions unique to them can very well be accounted. However, this is not entirely sufficient as, in general, two fixed orientations can themselves have different interfacial energies depending on the face along which they meet. Such kind of effects are not captured by Eq. (2). In spite of this, we still work with this so-called "isotropic grain growth model" for its simplicity and the fact that it was massively adopted before for the investigation of grain growth phenomenon [45–51]. Also, in situations where such anisotropy effects are indeed not that important, and other physics play a dominant role, like for example the interplay of interfacial tension and the counter diffusional fluxes in the problem of directional eutectic growth, Eq. (2) appears as one of the central pieces in their governing set of equations. That is, the current model serves as a base for a number of more advanced multiphase multicomponent microstructural evolution models. Before moving on to such coupled systems, it is only natural that we dispose of the simpler case, and hence, we choose Eq. (2) for our present asymptotic studies. For brevity, in the rest of the article, we use the term "phase" synonymously with "orientation."

In Ref. [43], Eq. (2) was studied in two spatial dimensions for its asymptotic behavior in the limit of the interface width specifier ϵ tending to zero. However, the outer analysis and the inner one pertaining to the binary interfaces were only performed. That is, the characteristics of the phase-field profile in the interiors of the grain bulks are first determined, and then, the same is carried out for open-strips around the binary interfaces. These regions are exemplarily illustrated in Fig. 1 which shows a schematic of five grains meeting to form a junction. The interior of one of the grain bulks is indicated by B, and a strip around a small portion of one of the interfaces by I, in Fig. 1. As part of the inner analysis within the binary interface strips, the next-to-the-leading-order equations are also studied in Ref. [43], and the (asymptotic or the limiting) kinetics of interface evolution is determined. In the current study, we take up from where we have left, and perform a detailed local analysis of the junctions (region J in Fig. 1, for example). This enables a determination of the characteristics of the phase indicator field (more concretely, the interfacial arrangement) within the junction neighborhoods and also the dynamics of motion of the common meeting point.

Let us consider a junction formed by M meeting interfaces (i.e., for the example case shown in Fig. 1, $M = 5$). Tangents to each of the involving binary interfaces can be drawn at the common meeting point, and rays can be attached to these, resulting in a structure that resembles a free body diagram of a point mass as depicted in Fig. 2(a), especially when the lengths are chosen proportional to the associated interfacial energies. As time passes, these rays can move apart or towards each other or rotate in unison about the point of their origin, depending on the dynamics. Thus, the motion of the junction is marked by the position and velocity of the center, while the motion of the interfaces relative to it by the evolution of the ray diagram. In the local analysis corresponding to the junctions to be carried out presently, the question of what kind of ray diagrams are permissible can be addressed. For example, is it possible to have three interfaces orienting themselves at any instant of time during the course of their evolution in such a way that their ray diagram is as in Fig. 2(b)? Can a junction between three phases with interfacial energies of 1, 2, and 4 units between them exhibit a stable motion? Such questions can be answered with the help of the analysis that follows. Furthermore, the influence of the bulk energies, the curvatures of the interfaces, and the interface mobilities on the instantaneous velocity of the center can also be estimated.

A. Local analysis of junctions

For performing the inner analysis, appropriate local coordinates have to be selected. We choose them in the following manner: Let (x, y, t) be the laboratory frame of reference in terms of which Eq. (2) has been written down. If $(x_*(t), y_*(t))$

marks the trajectory of the junction, then a change of axis $(x, y, t) \to (\zeta, \xi, t)$ is made such that $\zeta = \frac{x - x_*(t)}{\epsilon}$ and $\xi = \frac{y - y_*(t)}{\epsilon}$. This (ζ, ξ, t) will be the local coordinate system for our inner analysis around the junctions (see Fig. 1, for example). That is, the origin is shifted to coincide with the junction and the x and y axes are stretched by ϵ times to form the inner coordinates. As will be seen, it will also be quite rewarding to re-express the solutions in terms of coordinate axes obtained by rotating the ζ-ξ frame so as to align the ζ axis with the tangents of the interfaces at the confluence. If the local frame (ζ, ξ) is rotated to orient with the ith interface encountered when moving in the counter clockwise direction from the ζ axis, then the resultant coordinates are indicated using a suffix marking the interface, i.e., (ζ_i, ξ_i) (this is exemplified with (ζ_2, ξ_2) for the second interface in Fig. 1). Thus,

$$\begin{bmatrix} \zeta_i \\ \xi_i \end{bmatrix} = \begin{bmatrix} \cos\theta_i(t) & \sin\theta_i(t) \\ -\sin\theta_i(t) & \cos\theta_i(t) \end{bmatrix} \begin{bmatrix} \zeta \\ \xi \end{bmatrix}, \tag{3}$$

where $\theta_i(t)$ is the angle subtended at time t by the ith interface (encountered while moving in counter clockwise direction) with the ζ axis (which, in turn, is aligned with the laboratory frame's x axis (see Fig. 1).

Expressing the governing equation Eq. (2) in terms of the inner coordinates gives

$$\begin{aligned} \tau(\hat{\phi})\left(-\frac{v_x}{\epsilon}\frac{\partial\hat{\phi}_\beta}{\partial\zeta} - \frac{v_y}{\epsilon}\frac{\partial\hat{\phi}_\beta}{\partial\xi} + \frac{\partial\hat{\phi}_\beta}{\partial t}\right) \\ = -\frac{1}{\epsilon}f_\alpha\frac{\partial g_\alpha(\phi)}{\partial\phi_\beta}(\hat{\phi}) - \frac{1}{\epsilon^2}\gamma\frac{\partial W(\phi)}{\partial\phi_\beta}(\hat{\phi}) \\ + \frac{1}{\epsilon^2}\gamma\left(\frac{\partial^2\hat{\phi}_\beta}{\partial\zeta^2} + \frac{\partial^2\hat{\phi}_\beta}{\partial\xi^2}\right) - \hat{\lambda}, \quad \beta \in \{1, 2, \cdots, N\}, \end{aligned} \tag{4}$$

where $\hat{\phi}$ is the phase indicator field expressed in terms of the local coordinate system, i.e., by definition, $\hat{\phi}(\zeta, \xi, t; \epsilon) = \phi(x(\zeta, \xi, t), y(\zeta, \xi, t), t; \epsilon) = \phi(\epsilon\zeta + x_*(t), \epsilon\xi + y_*(t), t; \epsilon)$. The terms v_x and v_y are the x and y components of the instantaneous velocity of the junction point, i.e., $v_x = \frac{d}{dt}x_*(t)$ and $v_y = \frac{d}{dt}y_*(t)$. $\hat{\lambda}$ is the Lagrange parameter in the new coordinate system.

Next, $\hat{\phi}$, v_x, and v_y are assumed to posses asymptotic expansions of the Poincare type in the limit of ϵ vanishing:

$$\begin{aligned} \hat{\phi}(\zeta, \xi, t; \epsilon) \sim \hat{\phi}^{(0)}(\zeta, \xi, t) + \epsilon\hat{\phi}^{(1)}(\zeta, \xi, t) \\ + \epsilon^2\hat{\phi}^{(2)}(\zeta, \xi, t)\cdots, \end{aligned} \tag{5a}$$

$$v_x(t; \epsilon) \sim v_x^{(0)}(t) + \epsilon v_x^{(1)}(t) + \epsilon^2 v_x^{(2)}(t) + \cdots, \text{ and} \tag{5b}$$

$$v_y(t; \epsilon) \sim v_y^{(0)}(t) + \epsilon v_y^{(1)}(t) + \epsilon^2 v_y^{(2)}(t) + \cdots. \tag{5c}$$

These are substituted in Eq. (4) and the resultant is analyzed order by order to predict the configuration around the junction and also its kinetics of evolution. Of significant role in this step is the utilization of the boundary conditions at infinity satisfied by the terms of the asymptotic series of various orders like $\hat{\phi}^{(0)}$, $\hat{\phi}^{(1)}$, etc. These are provided by the matching relations.

In the case of binary interfaces, the outer expansions which pertain to the bulk interiors are taken to be of the following form

$$\begin{aligned} \phi(x, y, t; \epsilon) \sim \phi^{(0)}(x, y, t) + \epsilon\phi^{(1)}(x, y, t) \\ + \epsilon^2\phi^{(2)}(x, y, t) + \cdots. \end{aligned}$$

On the other hand, the local solution, defined as $\widetilde{\phi}(s, \rho, t) = \phi(x(s, \epsilon\rho, t), y(s, \epsilon\rho, t), t; \epsilon)$, is assumed to be expressible as an asymptotic series in the form

$$\begin{aligned} \widetilde{\phi}(s, \rho, t; \epsilon) \sim \widetilde{\phi}^{(0)}(s, \rho, t) + \epsilon\widetilde{\phi}^{(1)}(s, \rho, t) \\ + \epsilon^2\widetilde{\phi}^{(2)}(s, \rho, t) + \cdots, \end{aligned}$$

where (s, r) are the natural coordinates pertaining to the interface under question, with s being the arc length parameter of the base contour (see Ref. [43] for further details) and r, the distance along the normals to it; ρ is the stretched distance given by $\rho = r/\epsilon$. The matching relations which are popularly used for connecting the terms of these two asymptotic series are

$$\lim_{\rho\to\pm\infty}\widetilde{\phi}^{(0)}(s, \rho, t) = \lim_{r\to\pm 0}\phi^{(0)}(s, r, t) \quad \text{and} \tag{6}$$

$$\widetilde{\phi}^{(1)}(s, \rho, t) = \lim_{r\to\pm 0}\left(\phi^{(1)}(s, r, t) + \rho\frac{\partial\phi^{(0)}}{\partial r}(s, r, t)\right) + o(1) \quad \text{as} \rho \to \pm\infty, \tag{7}$$

where $\phi^{(0)}(s, r, t) := \phi^{(0)}(x(s, r, t), y(s, r, t), t)$ and $\phi^{(1)}(s, r, t) := \phi^{(1)}(x(s, r, t), y(s, r, t), t)$. That is, for every s, the $\rho \to \infty$ limit of the inner solution terms are matched to the $r \to 0$ limit of the outer ones.

However, the situation is not so simple when it comes to the matching exercise for the junctions. This is because, the inner expansions pertaining to the binary interfaces themselves act as outer ones along with those of the bulks when viewed from the standpoint of junctions. That is, the local solutions have to be matched with different functions along different directions. For instance, if infinity is to be approached always steering clear of the ζ_i axis exactly by a distance of ξ_* units, then the following relations should hold true:

$$\lim_{\zeta_i\to\infty}\hat{\phi}^{(0)}(\zeta_i, \xi_i = \xi_*) = \lim_{s\to 0}{}^i\widetilde{\phi}^{(0)}(s, \rho = \xi_*) \quad \text{and} \tag{8}$$

$$\hat{\phi}^{(1)}(\zeta_i, \xi_i = \xi_*) = \lim_{s\to 0}\left({}^i\widetilde{\phi}^{(1)}(s, \rho = \xi_*) + \zeta_i\frac{\partial\,{}^i\widetilde{\phi}^{(0)}}{\partial s}(s, \rho = \xi_*) + \left(\frac{-\kappa_{0,i}\zeta_i^2}{2}\right)\frac{\partial\,{}^i\widetilde{\phi}^{(0)}}{\partial\rho}(s, \rho = \xi_*)\right) + o(1) \quad \text{as } \zeta_i \to \infty, \tag{9}$$

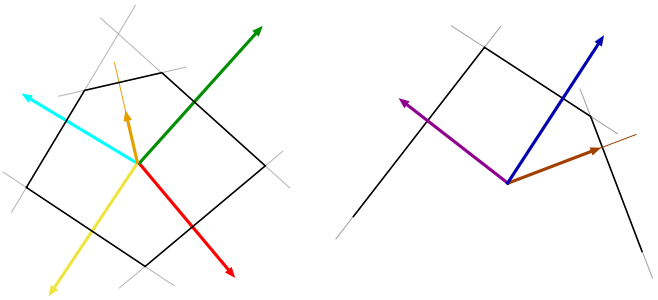

(a) (b)

FIG. 3. Polygonal constructions for the ray diagrams of Fig. 2. Panel (a) corresponds to Fig. 2(a), while panel (b) corresponds to Fig. 2(b).

where ${}^{i}\widetilde{\phi}^{(0)}$ and ${}^{i}\widetilde{\phi}^{(1)}$ are, respectively, the zeroth- and the first-order terms in the local expansion pertaining to the ith interface; $s = 0$ is taken to coincide with the junction point; the time dependence is suppressed for brevity; $\kappa_{0,i}$ is the curvature of the ith interface at the junction with the convention that a function in the (ζ_i, ξ_i) coordinate system (say $\xi_i = \xi_i(\zeta_i)$) which is concave upwards is positively curved; and, $\hat{\phi}^{(0)}(\zeta_i, \xi_i, t) := \hat{\phi}^{(0)}(\zeta(\zeta_i, \xi_i, t), \xi(\zeta_i, \xi_i, t), t)$ and $\hat{\phi}^{(1)}(\zeta_i, \xi_i, t) := \hat{\phi}^{(1)}(\zeta(\zeta_i, \xi_i, t), \xi(\zeta_i, \xi_i, t), t)$. A separate section (Sec. III) will be dedicated for the derivation of these matching conditions. The postponement is to avoid interruption to the flow of the local analysis that is being carried out. However, we do mention that Eq. (9) is a nontrivial statement, and it cannot be easily written down without due analysis. A naive extension of the matching relation Eq. (7) to the case of junctions is not sufficient to arrive at it as the last summand in the limit on the r.h.s. cannot be inferred through such a route. The actual way in which this term arises is given a detailed consideration in Sec. III; for now, we proceed with the leading-order analysis of the junctions. However, before starting, it is worth recalling a well familiar fact: The s dependence of Eqs. (8) and (9) (although present in the most generic of the cases) is unimportant for the current problem of interest, namely, the multiphase Allen-Cahn equation, Eq. (2). This is because, the zeroth and the first-order terms of the local expansions pertaining to the binary interfaces, i.e., $\widetilde{\phi}^{(0)}$ and $\widetilde{\phi}^{(1)}$, are independent of s for this problem.

1. Leading-order analysis

After substituting Eq. (5) in Eq. (4) and separating the orders, the leading-order requirement will be

$$\begin{bmatrix} 0 \\ 0 \\ . \\ . \\ . \\ 0 \end{bmatrix} = \begin{bmatrix} 1-\frac{1}{N} & -\frac{1}{N} & \dots & -\frac{1}{N} \\ -\frac{1}{N} & 1-\frac{1}{N} & \dots & -\frac{1}{N} \\ . & . & \dots & . \\ . & . & \dots & . \\ . & . & \dots & . \\ -\frac{1}{N} & -\frac{1}{N} & \dots & 1-\frac{1}{N} \end{bmatrix} \begin{bmatrix} \frac{\partial W(\phi)}{\partial \phi_1}(\hat{\phi}^{(0)}) - \left(\frac{\partial^2 \hat{\phi}_1^{(0)}}{\partial \zeta^2} + \frac{\partial^2 \hat{\phi}_1^{(0)}}{\partial \xi^2}\right) \\ \frac{\partial W(\phi)}{\partial \phi_2}(\hat{\phi}^{(0)}) - \left(\frac{\partial^2 \hat{\phi}_2^{(0)}}{\partial \zeta^2} + \frac{\partial^2 \hat{\phi}_2^{(0)}}{\partial \xi^2}\right) \\ . \\ . \\ . \\ \frac{\partial W(\phi)}{\partial \phi_N}(\hat{\phi}^{(0)}) - \left(\frac{\partial^2 \hat{\phi}_N^{(0)}}{\partial \zeta^2} + \frac{\partial^2 \hat{\phi}_N^{(0)}}{\partial \xi^2}\right) \end{bmatrix}. \tag{10}$$

The above equation has to be fulfilled in all of the $\mathbb{R}^2$ space; however, to begin with, we consider a smaller region which is then enlarged to equal the whole space. To construct the region, the associated ray diagrams will be used. Perpendiculars are drawn to the rays at equal distance σ from the center. When the innermost envelope of these lines forms a closed figure, for example like in Fig. 3(a), then that becomes the required region. However, when a closed figure does not form, as for the case of the ray diagram of Fig. 2(b), as illustrated in Fig. 3(b), the figure is closed by arbitrarily drawing a line to join the two hanging edges. Thus, the region in which Eq. (10) is considered is a closed convex polygon with the number of sides equal to or one greater than the number of interfaces. For the moment, the former case is considered; the adjustments for moving on to the latter are straightforward, as will become apparent shortly. The polygonal region of "size" σ will be denoted by the symbol $\hexagon_\sigma$ and its boundary by $\partial\hexagon_\sigma$ in the subsequent analysis.

In the next step, Eq. (10) is left multiplied with $\left(\frac{\partial \hat{\phi}_1^{(0)}}{\partial \zeta} \quad \frac{\partial \hat{\phi}_2^{(0)}}{\partial \zeta} \quad \dots \quad \frac{\partial \hat{\phi}_N^{(0)}}{\partial \zeta}\right)$, which will lead to the following owing to the initial filling satisfying the summation rule throughout the domain and its subsequent preservation through Lagrange multiplier implementation:

$$\left(\frac{\partial^2 \hat{\phi}_\alpha^{(0)}}{\partial \zeta^2} + \frac{\partial^2 \hat{\phi}_\alpha^{(0)}}{\partial \xi^2}\right)\frac{\partial \hat{\phi}_\alpha^{(0)}}{\partial \zeta} = \frac{\partial W(\phi)}{\partial \phi_\alpha}(\hat{\phi}^{(0)})\frac{\partial \hat{\phi}_\alpha^{(0)}}{\partial \zeta}. \tag{11}$$

In the above equation, as well as the following steps, the Einstein's convention (of summation over repeated indices) is used with (and only with) regard to the index α. In the next step, Eq. (11) is integrated over the polygonal region that is just

constructed:

$$\int_{\hexagon_\sigma} \frac{\partial^2 \hat{\phi}_\alpha^{(0)}}{\partial \zeta^2} \frac{\partial \hat{\phi}_\alpha^{(0)}}{\partial \zeta} dV + \int_{\hexagon_\sigma} \frac{\partial^2 \hat{\phi}_\alpha^{(0)}}{\partial \xi^2} \frac{\partial \hat{\phi}_\alpha^{(0)}}{\partial \zeta} dV = \int_{\hexagon_\sigma} \frac{\partial W(\hat{\phi}^{(0)})}{\partial \zeta} dV$$

$$\Rightarrow \frac{1}{2} \int_{\hexagon_\sigma} \frac{\partial}{\partial \zeta} \left(\frac{\partial \hat{\phi}_\alpha^{(0)}}{\partial \zeta} \frac{\partial \hat{\phi}_\alpha^{(0)}}{\partial \zeta} \right) dV + \int_{\hexagon_\sigma} \frac{\partial}{\partial \xi} \left(\frac{\partial \hat{\phi}_\alpha^{(0)}}{\partial \xi} \frac{\partial \hat{\phi}_\alpha^{(0)}}{\partial \zeta} \right) dV - \int_{\hexagon_\sigma} \frac{\partial \hat{\phi}_\alpha^{(0)}}{\partial \xi} \frac{\partial^2 \hat{\phi}_\alpha^{(0)}}{\partial \xi \partial \zeta} dV = \int_{\hexagon_\sigma} \frac{\partial W(\hat{\phi}^{(0)})}{\partial \zeta} dV$$

$$\Rightarrow \frac{1}{2} \int_{\hexagon_\sigma} \frac{\partial}{\partial \zeta} \left(\frac{\partial \hat{\phi}_\alpha^{(0)}}{\partial \zeta} \frac{\partial \hat{\phi}_\alpha^{(0)}}{\partial \zeta} \right) dV + \int_{\hexagon_\sigma} \frac{\partial}{\partial \xi} \left(\frac{\partial \hat{\phi}_\alpha^{(0)}}{\partial \xi} \frac{\partial \hat{\phi}_\alpha^{(0)}}{\partial \zeta} \right) dV - \frac{1}{2} \int_{\hexagon_\sigma} \frac{\partial}{\partial \zeta} \left(\frac{\partial \hat{\phi}_\alpha^{(0)}}{\partial \xi} \frac{\partial \hat{\phi}_\alpha^{(0)}}{\partial \xi} \right) dV = \int_{\hexagon_\sigma} \frac{\partial W(\hat{\phi}^{(0)})}{\partial \zeta} dV$$

$$\Rightarrow \int_{\hexagon_\sigma} \frac{\partial}{\partial \xi} \left(\frac{\partial \hat{\phi}_\alpha^{(0)}}{\partial \xi} \frac{\partial \hat{\phi}_\alpha^{(0)}}{\partial \zeta} \right) dV = \int_{\hexagon_\sigma} \frac{\partial}{\partial \zeta} \left\{ W(\hat{\phi}^{(0)}) + \frac{1}{2} \left(\frac{\partial \hat{\phi}_\alpha^{(0)}}{\partial \xi} \frac{\partial \hat{\phi}_\alpha^{(0)}}{\partial \xi} \right) - \frac{1}{2} \left(\frac{\partial \hat{\phi}_\alpha^{(0)}}{\partial \zeta} \frac{\partial \hat{\phi}_\alpha^{(0)}}{\partial \zeta} \right) \right\} dV.$$

Applying the divergence theorem to the above equation leads to

$$\int_{\partial \hexagon_\sigma} \frac{\partial \hat{\phi}_\alpha^{(0)}}{\partial \xi} \frac{\partial \hat{\phi}_\alpha^{(0)}}{\partial \zeta} \mathbf{n} \cdot \hat{\xi} dS = \int_{\partial \hexagon_\sigma} \left\{ W(\hat{\phi}^{(0)}) + \frac{1}{2} \left(\frac{\partial \hat{\phi}_\alpha^{(0)}}{\partial \xi} \frac{\partial \hat{\phi}_\alpha^{(0)}}{\partial \xi} \right) - \frac{1}{2} \left(\frac{\partial \hat{\phi}_\alpha^{(0)}}{\partial \zeta} \frac{\partial \hat{\phi}_\alpha^{(0)}}{\partial \zeta} \right) \right\} \mathbf{n} \cdot \hat{\zeta} dS$$

$$\Rightarrow \sum_{i=1}^{M} \int_{\partial(i)} \frac{\partial \hat{\phi}_\alpha^{(0)}}{\partial \xi} \frac{\partial \hat{\phi}_\alpha^{(0)}}{\partial \zeta} \mathbf{n} \cdot \hat{\xi} dS = \sum_{i=1}^{M} \int_{\partial(i)} \left\{ W(\hat{\phi}^{(0)}) + \frac{1}{2} \left(\frac{\partial \hat{\phi}_\alpha^{(0)}}{\partial \xi} \frac{\partial \hat{\phi}_\alpha^{(0)}}{\partial \xi} \right) - \frac{1}{2} \left(\frac{\partial \hat{\phi}_\alpha^{(0)}}{\partial \zeta} \frac{\partial \hat{\phi}_\alpha^{(0)}}{\partial \zeta} \right) \right\} \mathbf{n} \cdot \hat{\zeta} dS, \tag{12}$$

where $\partial(i)$ is the ith side of the polygon that was formed from the perpendicular drawn to the tangent to the ith interface. For any single such side, the contribution from it to the left-hand side (l.h.s.) when expressed in the coordinates oriented along the associated interface, i.e., (ζ_i, ξ_i) is

$$\int_{\partial(i)} \left(\frac{\partial \hat{\phi}_\alpha^{(0)}}{\partial \xi_i} \frac{\partial \xi_i}{\partial \xi} + \frac{\partial \hat{\phi}_\alpha^{(0)}}{\partial \zeta_i} \frac{\partial \zeta_i}{\partial \xi} \right) \left(\frac{\partial \hat{\phi}_\alpha^{(0)}}{\partial \xi_i} \frac{\partial \xi_i}{\partial \zeta} + \frac{\partial \hat{\phi}_\alpha^{(0)}}{\partial \zeta_i} \frac{\partial \zeta_i}{\partial \zeta} \right) \mathbf{n} \cdot \hat{\xi} dS. \tag{13}$$

In the limit of the size of the polygon becoming arbitrarily large, due to the matching relation Eq. (8), $\frac{\partial \hat{\phi}_\alpha^{(0)}}{\partial \zeta_i}$ vanishes. Therefore, the above integral reduces to

$$\int_{\substack{\partial(i) \\ \sigma \to \infty}} \left(\frac{\partial \hat{\phi}_\alpha^{(0)}}{\partial \xi_i} \frac{\partial \xi_i}{\partial \xi} \right) \left(\frac{\partial \hat{\phi}_\alpha^{(0)}}{\partial \xi_i} \frac{\partial \xi_i}{\partial \zeta} \right) \mathbf{n} \cdot \hat{\xi} dS = \int_{\substack{\partial(i) \\ \sigma \to \infty}} \frac{\partial \hat{\phi}_\alpha^{(0)}}{\partial \xi_i} \frac{\partial \hat{\phi}_\alpha^{(0)}}{\partial \xi_i} \cos\theta_i (-\sin\theta_i) \mathbf{n} \cdot \hat{\xi} dS. \tag{14}$$

Similarly, the r.h.s. of Eq. (12), as well, modifies in the like manner, together yielding

$$-\sum_{i=1}^{M} \int_{\substack{\partial(i) \\ \sigma \to \infty}} \frac{\partial \hat{\phi}_\alpha^{(0)}}{\partial \xi_i} \frac{\partial \hat{\phi}_\alpha^{(0)}}{\partial \xi_i} \cos\theta_i \sin\theta_i \mathbf{n} \cdot \hat{\xi} dS$$

$$= \sum_{i=1}^{M} \int_{\substack{\partial(i) \\ \sigma \to \infty}} \left\{ W(\hat{\phi}^{(0)}) + \frac{1}{2} \left(\frac{\partial \hat{\phi}_\alpha^{(0)}}{\partial \xi_i} \frac{\partial \hat{\phi}_\alpha^{(0)}}{\partial \xi_i} \right) \cos^2\theta_i - \frac{1}{2} \left(\frac{\partial \hat{\phi}_\alpha^{(0)}}{\partial \xi_i} \frac{\partial \hat{\phi}_\alpha^{(0)}}{\partial \xi_i} \right) \sin^2\theta_i \right\} \mathbf{n} \cdot \hat{\zeta} dS.$$

Since $\mathbf{n} \cdot \hat{\xi}$ and $\mathbf{n} \cdot \hat{\zeta}$ equal $\sin\theta_i$ and $\cos\theta_i$, respectively, the above equation simplifies to

$$\sum_{i=1}^{M} \int_{\substack{\partial(i) \\ \sigma \to \infty}} \left\{ W(\hat{\phi}^{(0)}) + \frac{1}{2} \left(\frac{\partial \hat{\phi}_\alpha^{(0)}}{\partial \xi_i} \frac{\partial \hat{\phi}_\alpha^{(0)}}{\partial \xi_i} \right) \cos^2\theta_i + \frac{1}{2} \left(\frac{\partial \hat{\phi}_\alpha^{(0)}}{\partial \xi_i} \frac{\partial \hat{\phi}_\alpha^{(0)}}{\partial \xi_i} \right) \sin^2\theta_i \right\} \cos\theta_i dS = 0$$

$$\Rightarrow \sum_{i=1}^{M} \int_{\substack{\partial(i) \\ \sigma \to \infty}} \left\{ W(\hat{\phi}^{(0)}) + \frac{1}{2} \left(\frac{\partial \hat{\phi}_\alpha^{(0)}}{\partial \xi_i} \frac{\partial \hat{\phi}_\alpha^{(0)}}{\partial \xi_i} \right) \right\} \cos\theta_i dS = 0. \tag{15}$$

However, owing to the matching relation Eq. (8), this means

$$\sum_{i=1}^{M} \int_{-\infty}^{\infty} \left\{ W({}^{i}\widetilde{\phi}^{(0)}) + \frac{1}{2} \left(\frac{\partial \, {}^{i}\widetilde{\phi}_\alpha^{(0)}}{\partial \rho} \frac{\partial \, {}^{i}\widetilde{\phi}_\alpha^{(0)}}{\partial \rho} \right) \right\} d\rho \cos\theta_i = 0. \tag{16}$$

The l.h.s. in this equation is nothing but the interfacial energy of the ith interface, except for the multiplicative factor of γ. Thus, multiplying Eq. (16) throughout with the latter gives

$$\sum_{i=1}^{M} (\text{I.E.})_i \cos\theta_i = 0, \tag{17}$$

where $(\text{I.E.})_i$ is the interfacial energy of the ith interface.

The adjustments to be made when one of the constructed sides does not correspond to any of the interfaces like, for instance, the "open side" of Fig. 3(b) are indeed trivial. Such a side eventually falls completely inside one of the bulks and thus $\hat{\phi}_\alpha^{(0)}$ saturates to a constant both with respect to ζ_i and ξ_i (see Sec. III B 3 for the rigorous argument). Further, the "value" it converges to corresponds to a minimum of the multiwell which is chosen to vanish. Thus, the contribution from this side to the sum on the l.h.s. of Eq. (15) is identically zero. The upshot being, the condition Eq. (17) with M being the number of interfaces meeting at a junction is a necessary requirement to be fulfilled by them at their common meeting point whether or not they give rise to a closed polygon.

Similarly, repeating the above procedure but by starting by left multiplying Eq. (10) with $(\frac{\partial\hat{\phi}_1^{(0)}}{\partial\xi} \quad \frac{\partial\hat{\phi}_2^{(0)}}{\partial\xi} \quad \dots \quad \frac{\partial\hat{\phi}_N^{(0)}}{\partial\xi})$ instead, leads to the following requirement:

$$\sum_{i=1}^{M} (\text{I.E.})_i \sin\theta_i = 0. \tag{18}$$

The conditions Eqs. (17) and (18) are reminiscent of the force balance requirement; the first one is the balance of ζ-components and the second that of ξ, with the interfacial energies taking the role of the applied forces. Therefore, the questions raised regarding the situations of Fig. 3(b) and the possibility of having a stable junction between interfaces with energies 1, 2, and 4 units is now easy to answer in the negative. This is because, in the former, it is impossible to balance out the y components of the "forces," while the latter don't satisfy the triangle inequality and hence cannot cancel themselves out. A corollary is that any ray diagram which does not produce a closed polygon upon the construction of the perpendiculars cannot be a valid solution: Note that the rays corresponding to the hanging edges have all the other rays lying only on one side of them, otherwise, their perpendiculars cannot be the ones hanging. Further, on the side to which the the other rays lie, the angle between them can at most be only 180°. Let the first ray make an angle of θ^* with the x axis. Then, since $\theta_i - \theta_*$ for all the interfaces is between 0° and 180°, and since all the $(\text{I.E.})_i$s are positive, we have

$$\sum_{i=1}^{M} (\text{I.E.})_i \sin(\theta_i - \theta_*) > 0$$
$$\Rightarrow \sum_{i=1}^{M} (\text{I.E.})_i \sin\theta_i \cos\theta_* - \sum_{i=1}^{M} (\text{I.E.})_i \cos\theta_i \sin\theta_* > 0.$$

Implying that Eqs. (17) and (18) cannot both be simultaneously satisfied for a construction that does not form a closed polygon. And since these equations represent the necessary conditions, such ray diagrams are never realized during the course of the evolution.

2. *Next-to-the-leading-order analysis*

We now proceed with the analysis at the next order. To begin with, the simpler case of the absence of driving forces, i.e., $f_\alpha = f_\beta \; \forall\, \alpha$ and β, or in particular, $f_\alpha = 0 \, \forall \, \alpha$, and the unit mobility case, i.e., $\tau(\phi) = 1$ will be considered. The interfacial energy multiplicative factor γ will also be taken to be unity. This will be generalized later. The corresponding equations at this order are

$$\begin{bmatrix} -v_x^{(0)}\frac{\partial\hat{\phi}_1^{(0)}}{\partial\zeta} - v_y^{(0)}\frac{\partial\hat{\phi}_1^{(0)}}{\partial\xi} \\ -v_x^{(0)}\frac{\partial\hat{\phi}_2^{(0)}}{\partial\zeta} - v_y^{(0)}\frac{\partial\hat{\phi}_2^{(0)}}{\partial\xi} \\ \vdots \\ -v_x^{(0)}\frac{\partial\hat{\phi}_N^{(0)}}{\partial\zeta} - v_y^{(0)}\frac{\partial\hat{\phi}_N^{(0)}}{\partial\xi} \end{bmatrix} = \begin{bmatrix} 1-\frac{1}{N} & -\frac{1}{N} & \dots & -\frac{1}{N} \\ -\frac{1}{N} & 1-\frac{1}{N} & \dots & -\frac{1}{N} \\ \vdots & \vdots & \dots & \vdots \\ -\frac{1}{N} & -\frac{1}{N} & \dots & 1-\frac{1}{N} \end{bmatrix} \begin{bmatrix} -\frac{\partial}{\partial\phi_\alpha}\frac{\partial W(\phi)}{\partial\phi_1}(\hat{\phi}^{(0)})\hat{\phi}_\alpha^{(1)} + \nabla^2\hat{\phi}_1^{(1)} \\ -\frac{\partial}{\partial\phi_\alpha}\frac{\partial W(\phi)}{\partial\phi_2}(\hat{\phi}^{(0)})\hat{\phi}_\alpha^{(1)} + \nabla^2\hat{\phi}_2^{(1)} \\ \vdots \\ -\frac{\partial}{\partial\phi_\alpha}\frac{\partial W(\phi)}{\partial\phi_N}(\hat{\phi}^{(0)})\hat{\phi}_\alpha^{(1)} + \nabla^2\hat{\phi}_N^{(1)} \end{bmatrix}, \tag{19}$$

where the operator ∇^2 is in terms of the local coordinates, i.e., ∇^2 stands for $\frac{\partial^2}{\partial\zeta^2} + \frac{\partial^2}{\partial\xi^2}$. Left multiplying the above with the row matrix $(\frac{\partial\hat{\phi}_1^{(0)}}{\partial\zeta} \quad \frac{\partial\hat{\phi}_2^{(0)}}{\partial\zeta} \quad \dots \quad \frac{\partial\hat{\phi}_N^{(0)}}{\partial\zeta})$ and integrating over the polygonal construction discussed previously gives

$$-v_x^{(0)}\int_{\hexagon_\sigma} \frac{\partial\hat{\phi}_\alpha^{(0)}}{\partial\zeta}\frac{\partial\hat{\phi}_\alpha^{(0)}}{\partial\zeta}dV - v_y^{(0)}\int_{\hexagon_\sigma} \frac{\partial\hat{\phi}_\alpha^{(0)}}{\partial\xi}\frac{\partial\hat{\phi}_\alpha^{(0)}}{\partial\zeta}dV = -\int_{\hexagon_\sigma} \frac{\partial}{\partial\phi_\alpha}\frac{\partial W(\phi)}{\partial\phi_\beta}(\hat{\phi}^{(0)})\hat{\phi}_\alpha^{(1)}\frac{\partial\hat{\phi}_\beta^{(0)}}{\partial\zeta}dV + \int_{\hexagon_\sigma} \nabla^2\hat{\phi}_\alpha^{(1)}\frac{\partial\hat{\phi}_\alpha^{(0)}}{\partial\zeta}dV,$$

where Einstein's summation convention is used with regard to the α and β indices. By the use of divergence theorem (twice), the last integral on the r.h.s. can be rewritten leading to

$$
\begin{aligned}
&- v_x^{(0)} \int_{\hexagon_\sigma} \frac{\partial \hat{\phi}_\alpha^{(0)}}{\partial \zeta} \frac{\partial \hat{\phi}_\alpha^{(0)}}{\partial \zeta} dV - v_y^{(0)} \int_{\hexagon_\sigma} \frac{\partial \hat{\phi}_\alpha^{(0)}}{\partial \xi} \frac{\partial \hat{\phi}_\alpha^{(0)}}{\partial \zeta} dV \\
&= - \int_{\hexagon_\sigma} \frac{\partial}{\partial \phi_\alpha} \frac{\partial W(\phi)}{\partial \phi_\beta} (\hat{\phi}^{(0)}) \hat{\phi}_\alpha^{(1)} \frac{\partial \hat{\phi}_\beta^{(0)}}{\partial \zeta} dV \\
&\quad + \int_{\hexagon_\sigma} \hat{\phi}_\alpha^{(1)} \nabla^2 \frac{\partial \hat{\phi}_\alpha^{(0)}}{\partial \zeta} dV \\
&\quad + \int_{\partial \hexagon_\sigma} \frac{\partial \hat{\phi}_\alpha^{(0)}}{\partial \zeta} \nabla \hat{\phi}_\alpha^{(1)} \cdot \mathbf{n} dS - \int_{\partial \hexagon_\sigma} \hat{\phi}_\alpha^{(1)} \nabla \frac{\partial \hat{\phi}_\alpha^{(0)}}{\partial \zeta} \cdot \mathbf{n} dS.
\end{aligned} \tag{20}
$$

To determine the second volume integral on the r.h.s. of the above equation, Eq. (10) is differentiated with respect to ζ, and the resultant is left multiplied with $(\hat{\phi}_1^{(1)} \quad \hat{\phi}_2^{(1)} \quad \dots \quad \hat{\phi}_N^{(1)})$ and subsequently integrated, resulting in

$$
\int_{\hexagon_\sigma} \hat{\phi}_\alpha^{(1)} \nabla^2 \frac{\partial \hat{\phi}_\alpha^{(0)}}{\partial \zeta} dV = \int_{\hexagon_\sigma} \frac{\partial}{\partial \zeta} \left(\frac{\partial W(\phi)}{\partial \phi_\alpha} (\hat{\phi}^{(0)}) \right) \hat{\phi}_\alpha^{(1)} dV,
$$

while the first volume integral on the r.h.s. can be manipulated in the following manner:

$$
\begin{aligned}
&\int_{\hexagon_\sigma} \frac{\partial}{\partial \phi_\alpha} \frac{\partial W(\phi)}{\partial \phi_\beta} (\hat{\phi}^{(0)}) \hat{\phi}_\alpha^{(1)} \frac{\partial \hat{\phi}_\beta^{(0)}}{\partial \zeta} dV \\
&= \int_{\hexagon_\sigma} \frac{\partial}{\partial \phi_\beta} \frac{\partial W(\phi)}{\partial \phi_\alpha} (\hat{\phi}^{(0)}) \hat{\phi}_\alpha^{(1)} \frac{\partial \hat{\phi}_\beta^{(0)}}{\partial \zeta} dV \\
&= \int_{\hexagon_\sigma} \frac{\partial}{\partial \phi_\beta} \frac{\partial W(\phi)}{\partial \phi_\alpha} (\hat{\phi}^{(0)}) \frac{\partial \hat{\phi}_\beta^{(0)}}{\partial \zeta} \hat{\phi}_\alpha^{(1)} dV \\
&= \int_{\hexagon_\sigma} \frac{\partial}{\partial \zeta} \left(\frac{\partial W(\phi)}{\partial \phi_\alpha} (\hat{\phi}^{(0)}) \right) \hat{\phi}_\alpha^{(1)} dV.
\end{aligned}
$$

Therefore, the first two terms on the r.h.s. of Eq. (20) cancel each other out leading to

$$
\begin{aligned}
&- v_x^{(0)} \int_{\hexagon_\sigma} \frac{\partial \hat{\phi}_\alpha^{(0)}}{\partial \zeta} \frac{\partial \hat{\phi}_\alpha^{(0)}}{\partial \zeta} dV - v_y^{(0)} \int_{\hexagon_\sigma} \frac{\partial \hat{\phi}_\alpha^{(0)}}{\partial \xi} \frac{\partial \hat{\phi}_\alpha^{(0)}}{\partial \zeta} dV \\
&= \int_{\partial \hexagon_\sigma} \frac{\partial \hat{\phi}_\alpha^{(0)}}{\partial \zeta} \nabla \hat{\phi}_\alpha^{(1)} \cdot \mathbf{n} dS - \int_{\partial \hexagon_\sigma} \hat{\phi}_\alpha^{(1)} \nabla \frac{\partial \hat{\phi}_\alpha^{(0)}}{\partial \zeta} \cdot \mathbf{n} dS.
\end{aligned} \tag{21}
$$

Similarly, repeating the analysis but by beginning by left multiplying Eq. (19) with $(\frac{\partial \hat{\phi}_1^{(0)}}{\partial \xi} \quad \frac{\partial \hat{\phi}_2^{(0)}}{\partial \xi} \quad \dots \quad \frac{\partial \hat{\phi}_N^{(0)}}{\partial \xi})$ instead, leads to

$$
\begin{aligned}
&- v_x^{(0)} \int_{\hexagon_\sigma} \frac{\partial \hat{\phi}_\alpha^{(0)}}{\partial \zeta} \frac{\partial \hat{\phi}_\alpha^{(0)}}{\partial \xi} dV - v_y^{(0)} \int_{\hexagon_\sigma} \frac{\partial \hat{\phi}_\alpha^{(0)}}{\partial \xi} \frac{\partial \hat{\phi}_\alpha^{(0)}}{\partial \xi} dV \\
&= \int_{\partial \hexagon_\sigma} \frac{\partial \hat{\phi}_\alpha^{(0)}}{\partial \xi} \nabla \hat{\phi}_\alpha^{(1)} \cdot \mathbf{n} dS - \int_{\partial \hexagon_\sigma} \hat{\phi}_\alpha^{(1)} \nabla \frac{\partial \hat{\phi}_\alpha^{(0)}}{\partial \xi} \cdot \mathbf{n} dS.
\end{aligned} \tag{22}
$$

The "surface integrals" appearing in Eqs. (21) and (22) can be categorized into two types: one containing the gradients of the partial derivatives of the zeroth order approximation, $\frac{\partial \hat{\phi}_\alpha^{(0)}}{\partial \zeta}$ and $\frac{\partial \hat{\phi}_\alpha^{(0)}}{\partial \xi}$, while the other that of the first-order correction, $\hat{\phi}^{(1)}$. Among these, the former can be shown to vanish identically due to the matching requirement Eq. (8) when the area of the polygon is made arbitrarily large. Considering explicitly the example of the rightmost integral of Eq. (22), we have

$$
\begin{aligned}
&\int_{\partial \hexagon_\sigma} \hat{\phi}_\alpha^{(1)} \nabla \frac{\partial \hat{\phi}_\alpha^{(0)}}{\partial \xi} \cdot \mathbf{n} dS \\
&= \sum_{i=1}^{M} \int_{\partial(i)} \hat{\phi}_\alpha^{(1)} \nabla \frac{\partial \hat{\phi}_\alpha^{(0)}}{\partial \xi} \cdot \mathbf{n} dS \\
&= \sum_{i=1}^{M} \int_{\partial(i)} \hat{\phi}_\alpha^{(1)} \left(\frac{\partial}{\partial \zeta} \frac{\partial \hat{\phi}_\alpha^{(0)}}{\partial \xi} \hat{\zeta} + \frac{\partial}{\partial \xi} \frac{\partial \hat{\phi}_\alpha^{(0)}}{\partial \xi} \hat{\xi} \right) \cdot \mathbf{n} dS \\
&= \sum_{i=1}^{M} \int_{\partial(i)} \hat{\phi}_\alpha^{(1)} \left(\frac{\partial}{\partial \zeta_i} \frac{\partial \hat{\phi}_\alpha^{(0)}}{\partial \xi} \hat{\zeta}_i + \frac{\partial}{\partial \xi_i} \frac{\partial \hat{\phi}_\alpha^{(0)}}{\partial \xi} \hat{\xi}_i \right) \cdot \mathbf{n} dS \\
&= \sum_{i=1}^{M} \int_{\partial(i)} \hat{\phi}_\alpha^{(1)} \left(\frac{\partial}{\partial \zeta_i} \frac{\partial \hat{\phi}_\alpha^{(0)}}{\partial \xi} \right) dS \\
&= \sum_{i=1}^{M} \int_{\partial(i)} \hat{\phi}_\alpha^{(1)} \left(\frac{\partial}{\partial \xi} \frac{\partial \hat{\phi}_\alpha^{(0)}}{\partial \zeta_i} \right) dS.
\end{aligned} \tag{23}
$$

However, in the limit that is of interest, $\hat{\phi}_\alpha^{(0)}$ approaches a constant value with regard to ζ_i (requirement of Eq. (8)), thus causing the derivative $\frac{\partial \hat{\phi}_\alpha^{(0)}}{\partial \zeta_i}$ to vanish, and thereby, the integral as a whole (please refer to Sec. IV B for the address of an associated crucial detail). In the same manner, the rightmost integral of Eq. (21) also vanishes.

Next, we look at the other type of integrals. Particularly, the first integral on the r.h.s. of Eq. (22) can be manipulated as

$$
\begin{aligned}
&\int_{\partial \hexagon_\sigma} \frac{\partial \hat{\phi}_\alpha^{(0)}}{\partial \xi} \nabla \hat{\phi}_\alpha^{(1)} \cdot \mathbf{n} dS \\
&= \sum_{i=1}^{M} \int_{\partial(i)} \frac{\partial \hat{\phi}_\alpha^{(0)}}{\partial \xi} \left(\frac{\partial}{\partial \zeta_i} \hat{\phi}_\alpha^{(1)} \hat{\zeta}_i + \frac{\partial}{\partial \xi_i} \hat{\phi}_\alpha^{(1)} \hat{\xi}_i \right) \cdot \mathbf{n} dS \\
&= \sum_{i=1}^{M} \int_{\partial(i)} \frac{\partial \hat{\phi}_\alpha^{(0)}}{\partial \xi} \frac{\partial \hat{\phi}_\alpha^{(1)}}{\partial \zeta_i} dS \\
&= \sum_{i=1}^{M} \int_{\partial(i)} \left(\frac{\partial \hat{\phi}_\alpha^{(0)}}{\partial \zeta_i} \frac{\partial \zeta_i}{\partial \xi} + \frac{\partial \hat{\phi}_\alpha^{(0)}}{\partial \xi_i} \frac{\partial \xi_i}{\partial \xi} \right) \frac{\partial \hat{\phi}_\alpha^{(1)}}{\partial \zeta_i} dS \\
&= \sum_{i=1}^{M} \frac{\partial \zeta_i}{\partial \xi} \int_{\partial(i)} \frac{\partial \hat{\phi}_\alpha^{(0)}}{\partial \zeta_i} \frac{\partial \hat{\phi}_\alpha^{(1)}}{\partial \zeta_i} dS \\
&\quad + \sum_{i=1}^{M} \frac{\partial \xi_i}{\partial \xi} \int_{\partial(i)} \frac{\partial \hat{\phi}_\alpha^{(0)}}{\partial \xi_i} \frac{\partial \hat{\phi}_\alpha^{(1)}}{\partial \zeta_i} dS.
\end{aligned} \tag{24}
$$

Dividing the above with the size of the polygon, i.e., the stretched distance σ at which the perpendiculars are drawn

on each tangent ray for constructing the polygon $\hexagon_\sigma$, gives

$$\begin{aligned}&\frac{1}{\sigma}\int_{\partial\hexagon_\sigma}\frac{\partial\hat{\phi}_\alpha^{(0)}}{\partial\xi}\nabla\hat{\phi}_\alpha^{(1)}\cdot\mathbf{n}dS\\&=\frac{1}{\sigma}\sum_{i=1}^{M}\frac{\partial\zeta_i}{\partial\xi}\int_{\partial(i)}\frac{\partial\hat{\phi}_\alpha^{(0)}}{\partial\zeta_i}\frac{\partial\hat{\phi}_\alpha^{(1)}}{\partial\zeta_i}dS\\&\quad+\frac{1}{\sigma}\sum_{i=1}^{M}\frac{\partial\xi_i}{\partial\xi}\int_{\partial(i)}\frac{\partial\hat{\phi}_\alpha^{(0)}}{\partial\xi_i}\frac{\partial\hat{\phi}_\alpha^{(1)}}{\partial\zeta_i}dS.\end{aligned}\tag{25}$$

Note that the polygon growing in size to eventually fill up the entire space is the same as $\sigma\to\infty$. In this limit, the first summand on the r.h.s. vanishes due to matching condition Eq. (8) and the exponential decay assumption (please refer to Sec. IV B). Further, by using, in addition, the other matching requirement, Eq. (9), as well, we will have

$$\begin{aligned}&\lim_{\sigma\to\infty}\frac{1}{\sigma}\sum_{i=1}^{M}\frac{\partial\xi_i}{\partial\xi}\int_{\partial(i)}\frac{\partial\hat{\phi}_\alpha^{(0)}}{\partial\xi_i}\frac{\partial\hat{\phi}_\alpha^{(1)}}{\partial\zeta_i}dS\\&=-\sum_{i=1}^{M}\frac{\partial\xi_i}{\partial\xi}\kappa_{0,i}\int_{-\infty}^{\infty}\frac{\partial\,{}^i\widetilde{\phi}^{(0)}}{\partial\rho}\frac{\partial\,{}^i\widetilde{\phi}^{(0)}}{\partial\rho}d\rho\end{aligned}\tag{26}$$

for the second summand. Similar arguments yield the following for the first integral on the r.h.s. of Eq. (21):

$$\begin{aligned}&\lim_{\sigma\to\infty}\frac{1}{\sigma}\int_{\partial\hexagon_\sigma}\frac{\partial\hat{\phi}_\alpha^{(0)}}{\partial\zeta}\nabla\hat{\phi}_\alpha^{(1)}\cdot\mathbf{n}dS\\&=-\sum_{i=1}^{M}\frac{\partial\xi_i}{\partial\zeta}\kappa_{0,i}\int_{-\infty}^{\infty}\frac{\partial\,{}^i\widetilde{\phi}^{(0)}}{\partial\rho}\frac{\partial\,{}^i\widetilde{\phi}^{(0)}}{\partial\rho}d\rho.\end{aligned}\tag{27}$$

Thus, emerging as the final outcome of the analysis at this order, the laws governing the trajectory of the junction are

$$\begin{aligned}&-v_x^{(0)}\lim_{\sigma\to\infty}\frac{1}{\sigma}\int_{\hexagon_\sigma}\frac{\partial\hat{\phi}_\alpha^{(0)}}{\partial\zeta}\frac{\partial\hat{\phi}_\alpha^{(0)}}{\partial\zeta}dV-v_y^{(0)}\\&\quad\times\lim_{\sigma\to\infty}\frac{1}{\sigma}\int_{\hexagon_\sigma}\frac{\partial\hat{\phi}_\alpha^{(0)}}{\partial\xi}\frac{\partial\hat{\phi}_\alpha^{(0)}}{\partial\zeta}dV=-\sum_{i=1}^{M}\frac{\partial\xi_i}{\partial\zeta}\kappa_{0,i}(\text{I.E.})_i\end{aligned}\tag{28}$$

and

$$\begin{aligned}&-v_x^{(0)}\lim_{\sigma\to\infty}\frac{1}{\sigma}\int_{\hexagon_\sigma}\frac{\partial\hat{\phi}_\alpha^{(0)}}{\partial\zeta}\frac{\partial\hat{\phi}_\alpha^{(0)}}{\partial\xi}dV-v_y^{(0)}\\&\quad\times\lim_{\sigma\to\infty}\frac{1}{\sigma}\int_{\hexagon_\sigma}\frac{\partial\hat{\phi}_\alpha^{(0)}}{\partial\xi}\frac{\partial\hat{\phi}_\alpha^{(0)}}{\partial\xi}dV=-\sum_{i=1}^{M}\frac{\partial\xi_i}{\partial\xi}\kappa_{0,i}(\text{I.E.})_i.\end{aligned}\tag{29}$$

The adjustments to be made for the case of a generic inverse mobility $\tau(\phi)$, arbitrary interfacial energy multiplicative factor γ, and the presence of bulk energies are straightforward, and the corresponding counterparts of Eqs. (28) and (29), respectively, read

$$\begin{aligned}&-v_x^{(0)}\lim_{\sigma\to\infty}\frac{1}{\sigma}\int_{\hexagon_\sigma}\tau(\hat{\phi}^{(0)})\frac{\partial\hat{\phi}_\alpha^{(0)}}{\partial\zeta}\frac{\partial\hat{\phi}_\alpha^{(0)}}{\partial\zeta}dV-v_y^{(0)}\\&\quad\times\lim_{\sigma\to\infty}\frac{1}{\sigma}\int_{\hexagon_\sigma}\tau(\hat{\phi}^{(0)})\frac{\partial\hat{\phi}_\alpha^{(0)}}{\partial\xi}\frac{\partial\hat{\phi}_\alpha^{(0)}}{\partial\zeta}dV\\&=-\lim_{\sigma\to\infty}\frac{1}{\sigma}\int_{\hexagon_\sigma}f_\alpha\frac{\partial}{\partial\zeta}g_\alpha(\hat{\phi}^{(0)})dV-\sum_{i=1}^{M}\frac{\partial\xi_i}{\partial\zeta}\kappa_{0,i}(\text{I.E.})_i\end{aligned}\tag{30}$$

and

$$\begin{aligned}&-v_x^{(0)}\lim_{\sigma\to\infty}\frac{1}{\sigma}\int_{\hexagon_\sigma}\tau(\hat{\phi}^{(0)})\frac{\partial\hat{\phi}_\alpha^{(0)}}{\partial\zeta}\frac{\partial\hat{\phi}_\alpha^{(0)}}{\partial\xi}dV-v_y^{(0)}\\&\quad\times\lim_{\sigma\to\infty}\frac{1}{\sigma}\int_{\hexagon_\sigma}\tau(\hat{\phi}^{(0)})\frac{\partial\hat{\phi}_\alpha^{(0)}}{\partial\xi}\frac{\partial\hat{\phi}_\alpha^{(0)}}{\partial\xi}dV\\&=-\lim_{\sigma\to\infty}\frac{1}{\sigma}\int_{\hexagon_\sigma}f_\alpha\frac{\partial}{\partial\xi}g_\alpha(\hat{\phi}^{(0)})dV-\sum_{i=1}^{M}\frac{\partial\xi_i}{\partial\xi}\kappa_{0,i}(\text{I.E.})_i.\end{aligned}\tag{31}$$

This concludes the next-to-the-leading-order calculations. Before proceeding to the discussion of the obtained results and some subtle aspects related to them, we dedicate a section to the derivation of the matching conditions.

III. DERIVATIONS OF THE MATCHING CONDITIONS

Matching relations take center stage in the asymptotic analysis of diffuse interface models. Understandably, they are very important as they serve to provide the boundary conditions (at infinity) to supplement the differential equations retrieved at various orders. In fact, sometimes, the obtained boundary value problems are not even solved, but still the sought after information about the performance of the models is extracted mainly by the help of the matching relations. This is very well known, for instance, in the next-to-the-leading-order local analysis of the famous scalar Allen-Cahn or Cahn-Hilliard etc. models; where, the kinetic laws of interfacial evolution are uncovered. We point out that even in the current analysis of junctions, in the leading order, it is predominantly by a clever exploitation of the matching conditions that the restrictions on the interfacial configurations at the junction points are derived as opposed to by actually analyzing the differential equations for their solutions. This is also true for the next order where the laws governing the junction's motion are derived. In spite of such being the significance of the role played by the matching conditions, their derivations, unfortunately, are not very popularly known. The authors are unaware of any work providing a detailed explanation of their emergence, even for the case of single boundary layer variable, i.e., the relations Eqs. (6) and (7) which are very widely used. The present section of the article is dedicated to address this shortage. We provide the derivations of the matching requirements satisfied by the terms of the inner expansions and the outer ones in the case of one-dimensional layers and also the zero-dimensional ones, i.e., junction points (we recall once again that only two-spatial dimensions are concerned with throughout the

current work). We assume a strong overlap hypothesis [52] for deriving the matching conditions.

A. Single boundary layer variable

The case of single boundary layer variable will be reviewed. It is this which corresponds to the matching relations relevant to the binary interfaces. However, for simplification, only a single independent variable is assumed. Let a function $\phi(r;\epsilon)$, $r \in [0,1]$ have a regular asymptotic expansion in terms of the (gauge) set $\{\epsilon^0, \epsilon^1, \epsilon^2, \cdots\}$ in the supremum norm in any interval of the form $[A,1]$ with $A > 0$. When expressed in terms of the stretched variable $\rho = r/\epsilon$, let the function be denoted by $\widetilde{\phi}(\rho;\epsilon)$ and let it have a regular expansion within the same set $\{\epsilon^0, \epsilon^1, \epsilon^2, \cdots\}$ in any interval of the form $[0,A]$ where $A > 0$. Hence, by extension theorems [52], we have the following:

For some $\nu > 0$ and $\mu > 0$,

$$\frac{\phi(r;\epsilon) - \phi^{(0)}(r)}{\epsilon} = \phi^{(1)}(r) + o(1) \text{ uniformly in } r \in [\epsilon^{\nu}, 1] \quad \text{and} \tag{32}$$

$$\frac{\widetilde{\phi}(\rho;\epsilon) - \widetilde{\phi}^{(0)}(\rho)}{\epsilon} = \widetilde{\phi}^{(1)}(\rho) + o(1) \text{ uniformly in } \rho \in \left[0, \frac{1}{\epsilon^{\mu}}\right]. \tag{33}$$

We assume strong overlap of the extended domains of validity, that is, $\epsilon^{\nu} < \epsilon^{1-\mu}$. If μ were to be greater than unity, then the local expansion alone approximates the function in the whole of the domain implying that the problem is not singular but regular, hence we take that $\mu < 1$. Equations (32) and (33) imply that if $\epsilon\phi^{(1)}(r) = o(1)$ uniformly in $r \in [\epsilon^{\nu}, 1]$ and $\epsilon\widetilde{\phi}^{(1)}(\rho) = o(1)$ uniformly in $\rho \in [0, \frac{1}{\epsilon^{\mu}}]$, then

$$\phi(r;\epsilon) = \phi^{(0)}(r) + o(1) \text{ uniformly in } r \in [\epsilon^{\nu}, 1] \quad \text{and} \tag{34}$$

$$\widetilde{\phi}(\rho;\epsilon) = \widetilde{\phi}^{(0)}(\rho) + o(1) \text{ uniformly in } \rho \in \left[0, \frac{1}{\epsilon^{\mu}}\right]. \tag{35}$$

Re-expressing the first of the above statements in terms of ρ gives

$$\phi(\epsilon\rho;\epsilon) = \phi^{(0)}(\epsilon\rho) + o(1) \text{ uniformly in } \rho \in [\epsilon^{\nu-1}, \epsilon^{-1}].$$

Since $\widetilde{\phi}(\rho;\epsilon)$ and $\phi(r;\epsilon)$ are the same quantity, for any $\rho \in [\epsilon^{\nu-1}, \epsilon^{-\mu}]$, we have

$$\begin{aligned} 0 &\leqslant |\widetilde{\phi}^{(0)}(\rho) - \phi^{(0)}(\epsilon\rho)| \\ &= |\widetilde{\phi}^{(0)}(\rho) - \widetilde{\phi}(\rho;\epsilon) + \phi(r;\epsilon) - \phi^{(0)}(\epsilon\rho)| \\ &\leqslant |\widetilde{\phi}^{(0)}(\rho) - \widetilde{\phi}(\rho;\epsilon)| + |\phi(\epsilon\rho;\epsilon) - \phi^{(0)}(\epsilon\rho)| \\ &\leqslant \sup_{\rho\in[\epsilon^{\nu-1},\epsilon^{-\mu}]} |\widetilde{\phi}^{(0)}(\rho) - \widetilde{\phi}(\rho;\epsilon)| \\ &\quad + \sup_{\rho\in[\epsilon^{\nu-1},\epsilon^{-\mu}]} |\phi(\epsilon\rho;\epsilon) - \phi^{(0)}(\epsilon\rho)|. \end{aligned}$$

In the limit of ϵ vanishing, because of Eqs. (34) and (35), we have

$$\lim_{\epsilon\to 0}(\widetilde{\phi}^{(0)}(\rho) - \phi^{(0)}(\epsilon\rho)) = 0 \text{ uniformly in } \rho \in [\epsilon^{\nu-1}, \epsilon^{-\mu}].$$

Since $0 < \nu < 1$ and $0 < \mu < 1$, this implies

$$\lim_{\rho\to\infty}\lim_{r\to 0^+}(\widetilde{\phi}^{(0)}(\rho) - \phi^{(0)}(r)) = 0.$$

That is,

$$\boxed{\lim_{\rho\to\infty}\widetilde{\phi}^{(0)}(\rho) = \lim_{r\to 0^+}\phi^{(0)}(r)}$$

if the limits exist. This is the matching condition for the zeroth order terms of the asymptotic expansion. Repeating the above calculations for the higher order corrections, that is, for Eqs. (32) and (33) we get

$$\lim_{\epsilon\to 0}\left(\widetilde{\phi}^{(1)}(\rho) - \phi^{(1)}(\epsilon\rho) - \rho\left.\frac{\partial\phi^{(0)}}{\partial r}\right|_{0^+} - \epsilon\rho^2\frac{1}{2}\left.\frac{\partial^2\phi^{(0)}}{\partial r^2}\right|_{r^*} + \frac{\widetilde{\phi}^{(0)}(\rho) - \phi^{(0)}(0^+)}{\epsilon}\right) = 0, \tag{36}$$

where $r^* \in (0, \epsilon^{1-\mu})$, $\rho \in [\epsilon^{\nu-1}, \epsilon^{-\mu}]$ and $\lim_{r\to 0^+}\frac{\partial\phi^{(0)}}{\partial r}$ is assumed to exist. However, instead of this relation, the following gained fame to be the matching condition for the first-order local correction:

$$\boxed{\widetilde{\phi}^{(1)}(\rho) = \phi^{(1)}(0^+) + \rho\left.\frac{\partial\phi^{(0)}}{\partial r}\right|_{0^+} + o(1) \text{ as } \rho\to\infty.}$$

That is, $\lim_{r\to 0^+}\phi^{(1)}(r)$ is assumed to exist, and the limit of the remaining terms is assumed to vanish, for instance, by $\lim_{\epsilon\to 0}(\widetilde{\phi}^{(0)}(\epsilon^{-\mu}) - \phi^{(0)}(0^+))$ approaching zero faster than ϵ, and $\lim_{\epsilon\to 0}\frac{\partial^2\phi^{(0)}}{\partial r^2}$ vanishing appropriately fast.

B. Two boundary layer variables

1. *Some specific examples*

Before beginning the derivation of the matching conditions, we look at some examples of functions exhibiting a junction behavior. Our first example is the following:

$$\Phi(x,y;\epsilon) = e^{-x/\epsilon} + e^{-y/\epsilon} \quad \forall x \geqslant 0,\ y \geqslant 0. \tag{37}$$

This function has the trivial function as the asymptotic approximation as $\epsilon \to 0$ when neither of x and y is zero. However, when one of them is zero, and the other is not, the constant function 1 is the asymptotic approximation. As a result, traveling towards the x axis along the dotted red line of Fig. 4(a) gives a limit of $\Phi(x,y;\epsilon) = 0$ as ϵ vanishes for any $y > 0$ but when y exactly equals zero, the limit is 1. Likewise is the behavior for any other vertical line except the y axis and also any horizontal line except the x axis. In other words, the function has boundary layers along the positive x and y axes of the kind considered in Sec. III A. Furthermore, when $x = 0$ and $y = 0$, the value of the function is 2 as $\epsilon \to 0$. Hence, it exhibits a junction behavior at the origin.

As a second example, traces of two curves $\mathscr{C}_1$ and $\mathscr{C}_2$, both of which containing the origin, are considered in the first quadrant as shown in Fig. 4(b). Then, for all the points on the paths and in the intermediate region between them (shaded region), the following function is defined:

$$\Phi(x,y;\epsilon) = e^{-r_1(x,y)/\epsilon} + e^{-r_2(x,y)/\epsilon}, \tag{38}$$

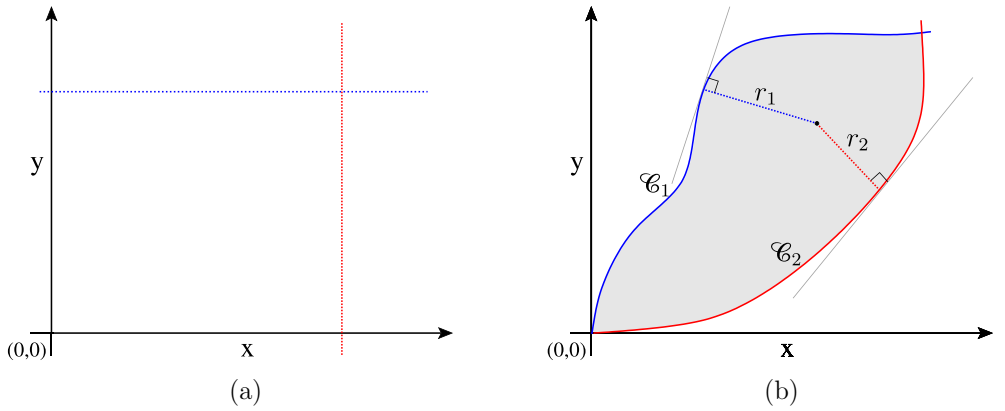

FIG. 4. Domains considered for some example functions exhibiting a junction behavior. Domain of (a) corresponds to the simplest function Eq. (37), while that in (b) is considered for the example in Eq. (38).

where $r_1(x, y)$ is the distance of the point (x, y) from the trace of the first curve and $r_2(x, y)$ is from that of the second. It is easy to see, as before, that this function exhibits boundary layers of the kind considered in Sec. III A along the paths except at origin where it shows a junction behavior.

2. *Study of asymptotic behavior of one of the considered examples*

Before deriving the matching relations in a generic fashion, it will be highly beneficial to be informed about what could be expected by studying the asymptotic behavior of a specific example. Particularly, Eq. (38) for the special case of the first trace coinciding with the y axis and the second one with that of the graph of a function $f(x)$ will be considered. That is, the function

$$\Phi(x, y; \epsilon) = e^{-x/\epsilon} + e^{-r(x,y)/\epsilon} \tag{39}$$

is studied, where $r(x, y)$ is the distance of the point (x, y) from the graph of $f(x)$. All $y \geqslant f(x)$ and the y axis constitute the domain of interest. Furthermore, let $f(x)$ be double differentiable with $f'(0) = 0$. Consider the natural coordinates associated with the graph of $f(x)$; namely, the distance along the graph s and the distance normal to it r. The latter is stretched to give $\rho = r/\epsilon$. We make a further choice that the former is measured from the origin. For simplicity, let us assume that all the points of the region of interest have a unique representation in the local coordinate system. This necessarily requires that $f''(x) \leqslant 0$. And we further demand that $f''(0) \neq 0$. A schematic drawing of a function $f(x)$ constructed in such a way is shown in Fig. 5. The shaded region ($x > 0$ and $y > f(x)$), the blue and the red paths constitute the domain of interest for the function of Eq. (39).

The function of Eq. (39) when re-expressed in the inner coordinates pertaining to the graph of $f(x)$ reads

$$\widetilde{\Phi}(s, \rho; \epsilon) = \Phi(x(s, \epsilon\rho), y(s, \epsilon\rho); \epsilon) = e^{-x(s,\epsilon\rho)/\epsilon} + e^{-\rho}.$$

Now, consider the regular asymptotic expansion of the above in the gauge set $\{\epsilon^0, \epsilon^1, \epsilon^2, \cdots\}$ and in any neighborhood not containing $s = 0$, i.e., for instance, in "rectangles" of (s, ρ) of the form $[A, 1] \times [0, B]$ $\forall A > 0$ and $B > 0$. Since $x(s, \epsilon\rho)$ is bounded below by a positive value as $\epsilon \to 0$ in these domains, the regular expansion in the considered gauge set has only one nontrivial term and that is the zeroth order contribution. Therefore, the asymptotic expansion of $\widetilde{\Phi}(s, \rho; \epsilon)$ is identically

$$\begin{aligned}\widetilde{\Phi}(s, \rho; \epsilon) &\sim \widetilde{\Phi}^{(0)}(s, \rho) + \epsilon\widetilde{\Phi}^{(1)}(s, \rho) + \epsilon^2\widetilde{\Phi}^{(2)}(s, \rho) + \cdots \\ &= e^{-\rho} + \epsilon 0 + \epsilon^2 0 + \cdots .\end{aligned}$$

Next, we consider the inner expansion associated with the junction. Let the stretched coordinates centered at the junction be $\zeta = x/\epsilon$ and $\xi = y/\epsilon$. The function $\Phi(x, y; \epsilon)$ in these coordinates is

$$\hat{\Phi}(\zeta, \xi; \epsilon) := \Phi(\epsilon\zeta, \epsilon\xi; \epsilon) = e^{-\zeta} + e^{-r(\epsilon\zeta, \epsilon\xi)/\epsilon}, \tag{40}$$

whose domain of interest is $\{(\zeta, \xi) \in \mathbb{R} : \zeta \in [0, \infty)$ and $\xi \geqslant f(\epsilon\zeta)/\epsilon\}$. Now we consider the regular asymptotic expansion of the above in the gauge set $\{\epsilon^0, \epsilon^1, \epsilon^2, \cdots\}$ in any neighborhood containing a segment of ξ axis and particularly in rectangles of (ζ, ξ) of the form $[0, A] \times [B, C]$ $\forall A > 0$ and $0 < B < C$. In these regions, the following is

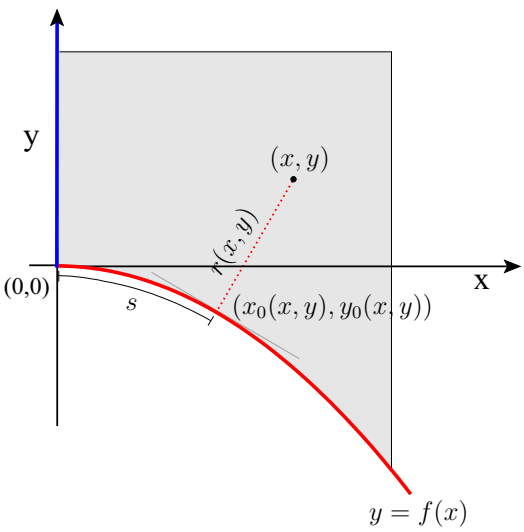

FIG. 5. Domain considered for the example function of Eq. (39).

analyzed:

$$r(x,y)=\sqrt{(x-x_0(x,y))^2+(y-y_0(x,y))^2}, \tag{41}$$

where $(x_0(x,y), y_0(x,y))$ is the nearest point of (x,y) on the graph of $f(x)$. Therefore, by definition, $y_0(x,y)=f(x_0(x,y))$ and

$$x_0-x=[y-f(x_0)]f'(x_0). \tag{42}$$

Hence, we have

$$\begin{aligned}
\frac{r(\epsilon\zeta,\epsilon\xi)}{\epsilon}&=\frac{1}{\epsilon}\sqrt{\{\epsilon\zeta-x_0(\epsilon\zeta,\epsilon\xi)\}^2+\{\epsilon\xi-f(x_0(\epsilon\zeta,\epsilon\xi))\}^2}\\
&=\frac{1}{\epsilon}\sqrt{(\{\epsilon\xi-f(x_0(\epsilon\zeta,\epsilon\xi))\}f'(x_0(\epsilon\zeta,\epsilon\xi)))^2+\{\epsilon\xi-f(x_0(\epsilon\zeta,\epsilon\xi))\}^2}\\
&=\frac{\epsilon\xi-f(x_0(\epsilon\zeta,\epsilon\xi))}{\epsilon}\sqrt{1+(f'(x_0(\epsilon\zeta,\epsilon\xi)))^2}\\
&=\frac{\epsilon\xi-\left\{f(0)+f'(0)x_0(\epsilon\zeta,\epsilon\xi)+\frac{f''(x_*)}{2}x_0^2(\epsilon\zeta,\epsilon\xi)\right\}}{\epsilon}\sqrt{1+\{f'(x_0(\epsilon\zeta,\epsilon\xi))\}^2}\\
&=\left\{\xi-\frac{f''(x_*)}{2\epsilon}x_0^2(\epsilon\zeta,\epsilon\xi)\right\}\sqrt{1+\{f'(x_0(\epsilon\zeta,\epsilon\xi))\}^2}\\
&=\left\{\xi-\frac{f''(x_*)}{2\epsilon}x_0^2(\epsilon\zeta,\epsilon\xi)\right\}\left\{1+\frac{f'(x_{**})f''(x_{**})}{\sqrt{1+[f''(x_{**})]^2}}x_0(\epsilon\zeta,\epsilon\xi)\right\}.
\end{aligned} \tag{43}$$

We now find estimates for the term $x_0(\epsilon\zeta,\epsilon\xi)$ of Eq. (43). Consider Eq. (42) for $x=\epsilon\zeta$ and $y=\epsilon\xi$:

$$\begin{aligned}
x_0&=\epsilon\zeta+(\epsilon\xi-f(x_0))f'(x_0) \qquad (44)\\
&=\epsilon\zeta+\left(\epsilon\xi-f(0)-f'(0)x_0-\frac{f''(x^*)}{2}x_0^2\right)\\
&\quad\times(f'(0)+f''(x^{**})x_0)\\
&=\epsilon\zeta+\left(\epsilon\xi-\frac{f''(x^*)}{2}x_0^2\right)f''(x^{**})x_0\\
\Rightarrow\epsilon\zeta&=(1-\epsilon\xi f''(x^{**}))x_0+\frac{f''(x^*)}{2}f''(x^{**})x_0^3. \qquad (45)
\end{aligned}$$

Furthermore, for $\zeta>0$, (it can be shown that) $0<x_0(\epsilon\zeta,\epsilon\xi)<\epsilon\zeta$, implying that $x_0(\epsilon\zeta,\epsilon\xi)\to 0$ as $\epsilon\to 0$. Also $x_0(0,\epsilon\xi)=0$. This means, from Eq. (45) we will have

$$\epsilon\zeta\geqslant(1-\epsilon\xi f''(x^{**}))x_0 \quad\text{and}$$

$$\epsilon\zeta\leqslant\left(1-\epsilon\xi f''(x^{**})+\frac{f''(x^*)}{2}f''(x^{**})\right)x_0$$

for small enough ϵ. That is

$$\frac{\epsilon\zeta}{\left(1-\epsilon\xi f''(x^{**})+\frac{f''(x^*)}{2}f''(x^{**})\right)}\leqslant x_0\leqslant\frac{\epsilon\zeta}{(1-\epsilon\xi f''(x^{**}))}.$$

Or in other words, $x_0/\epsilon\zeta=\mathcal{O}(1)$ as $\epsilon\to 0\ \forall\zeta>0$ due to the existence of $f''(0)$. From this, using limit laws, it follows from Eq. (45) that $\lim_{\epsilon\to 0}x_0/\epsilon=\zeta\ \ \forall\zeta\geqslant 0$. Therefore, Eq. (43) becomes

$$\begin{aligned}
\frac{r(\epsilon\zeta,\epsilon\xi)}{\epsilon}&=\left\{\xi-\epsilon\frac{f''(0)}{2}\zeta^2\right\}\\
&\quad\times\left\{1+\frac{o(1)f''(0)}{\sqrt{1+[f''(0)]^2}}\epsilon\zeta\right\}\quad\text{as}\quad\epsilon\to 0\\
\Rightarrow\frac{r(\epsilon\zeta,\epsilon\xi)}{\epsilon}&=\xi-\epsilon\frac{f''(0)}{2}\zeta^2+o(\epsilon).
\end{aligned}$$

Substituting this in Eq. (40) gives

$$\mathring{\Phi}(\zeta,\xi;\epsilon)=e^{-\zeta}+e^{-\xi}\left(1+\epsilon\frac{f''(0)}{2}\zeta^2+o(\epsilon)\right).$$

That is,

$$\mathring{\Phi}^{(0)}(\zeta,\xi)=e^{-\zeta}+e^{-\xi}\quad\text{and}$$

$$\mathring{\Phi}^{(1)}(\zeta,\xi)=e^{-\xi}\frac{f''(0)}{2}\zeta^2.$$

We now connect the local expansion terms pertaining to the junction point to those of the trace of the curve. Particularly, we can write the following:

$$\mathring{\Phi}^{(1)}(\zeta,\xi)=-\frac{\partial\widetilde{\Phi}^{(0)}(s,\rho)}{\partial\rho}(0,\xi)\frac{f''(0)}{2}\zeta^2. \tag{46}$$

That is, for the currently considered example, $\mathring{\Phi}^{(1)}$ has a square dependence with regard to the ζ variable, and it appears multiplied to the ρ derivative of $\widetilde{\Phi}^{(0)}$. However, it will be shown next that this is, in fact, generically true, albeit as $\zeta\to\infty$. In fact, the whole purpose of the above derivation has been to provide a concrete example that brings out the emergence of the square dependence more clearly as compared to the complicated derivation to follow.

3. *Matching relations for junction regions*

The derivation involves the exact same ideas as in Sec. III A, namely that asymptotic expansions are constructed along a path and in the junction neighbourhood in streched coordinates. Following this, an intersection of the domains of validity of the expansions is assumed, and the implications are pursued to arrive at the matching relations. However, the calculations are complicated by the fact that an additional stretched dimension is now present. Since the principal idea is the same, and the differences are only in the details, we

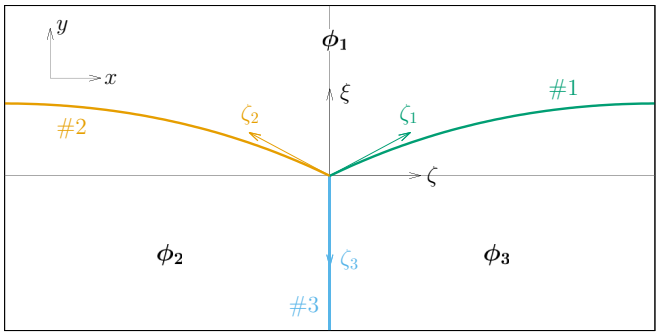

FIG. 6. Setup considered for demonstrating the accuracy of the asymptotic laws Eqs. (28) and (29) in predicting the instantaneous motion of a junction.

push the derivation of the two boundary layer variables case to Appendix A.

IV. DISCUSSION

A. Quadratic growth behavior

The importance of the term carrying ζ_i^2 in Eq. (9) cannot be over-emphasized. In the case of binary interfaces, the first-order correction $\widetilde{\phi}_\alpha^{(1)}(s,\rho)$ is not of the order ρ^2 as ρ approaches infinity. Eq. (7) only says that the outer limit of the first-order inner correction matches with the inner limit of the first-order outer correction plus inner variable times the inner limit of the derivative of the zeroth order term of the outer expansion. It would be tempting to extend this, in a naive way, to a higher order interior "layer," i.e., a neighborhood of a junction, in the following manner:

$$\hat{\phi}_\alpha^{(1)}(\zeta_i,\xi_i) = \lim_{s\to 0}\left(\widetilde{\phi}^{(1)}(s,\rho=\xi_i) + \zeta_i \frac{\partial \widetilde{\phi}^{(0)}}{\partial s}(s,\rho=\xi_i)\right) + o(1) \text{ as } \zeta_i \to \infty. \tag{47}$$

That is, without the ζ_i^2 dependence. Let us see what the predictions would be if the analysis of Sec. II A 2 is instead performed with this naive extension. As the local solution corresponding to the binary interfaces is independent of the distance along the interface in the problem we are concerned with, the second term on the r.h.s. of the above equation is identically zero. This implies that the calculation in Eq. (25) ultimately returns a vanishing value. That is, not only the integrals of the type considered in Eq. (23), but also of the kind analyzed in Eq. (25) vanish. Hence, Eqs. (21) and (22) will reduce to

$$-v_x^{(0)}\int_{\hexagon_\sigma}\frac{\partial\hat{\phi}_\alpha^{(0)}}{\partial\zeta}\frac{\partial\hat{\phi}_\alpha^{(0)}}{\partial\zeta}dV - v_y^{(0)}\int_{\hexagon_\sigma}\frac{\partial\hat{\phi}_\alpha^{(0)}}{\partial\xi}\frac{\partial\hat{\phi}_\alpha^{(0)}}{\partial\zeta}dV = 0 \tag{48}$$

and

$$-v_x^{(0)}\int_{\hexagon_\sigma}\frac{\partial\hat{\phi}_\alpha^{(0)}}{\partial\zeta}\frac{\partial\hat{\phi}_\alpha^{(0)}}{\partial\xi}dV - v_y^{(0)}\int_{\hexagon_\sigma}\frac{\partial\hat{\phi}_\alpha^{(0)}}{\partial\xi}\frac{\partial\hat{\phi}_\alpha^{(0)}}{\partial\xi}dV = 0. \tag{49}$$

Now consider the setup of Fig. 6 where three phases ϕ_1, ϕ_2, and ϕ_3 with equal bulk energies are in contact as shown. The interfaces 1 and 2 are mirror images of one another with regard to interface 3, and all the three have the same surface tension. Further, they always meet with the bounding box at necessarily right angles. Then, the evolution should progress in such a way that the triple junction moves only in the downward direction. The impossibility of the horizontal motion can be easily deduced from the symmetry considerations, and the downward direction for the vertical motion can be corroborated using the Gibbs-Thomson condition. However, if Eqs. (48) and (49) rightly predict a value of zero for v_x, then substituting it in the latter of the equations shows that they will wrongly predict a value of zero for v_y. Thus, writing down the matching relation for junctions without due analysis and just by mimicking the well known counterpart of the binary interfaces seriously falls short. The dependence of the instantaneous velocity of the junction on the instantaneous curvatures of the interfaces at the common meeting point is highly reasonable which is entirely a result of the ζ^2 term of the matching relation which warrants the analysis of Appendix A.

We make it a special point to emphasize once again that there is no counterpart to the ζ^2 term of Eq. (A25) in a single variable boundary layer case. For binary interfaces, there are two independent variables, s and ρ. But only one of them is the boundary layer variable namely ρ. Even if the matching laws are derived taking both s and ρ into account, a ρ^2 wouldn't arise being multiplied to first derivatives. On the other hand for a junction, the independent variables are also two in number, viz. ζ and ξ. However, both of them are boundary layer variables. Furthermore, here, one will find that ζ^2 appears multiplied to first ρ (or ξ) partial derivative. There is no option but to perform the analysis of Appendix A to realize this. And without this quadratic term, the equations of motion for junctions remain far from complete.

B. Exponential decay assumption

The discussion that the r.h.s. of Eq. (23) identically vanishes as the polygonal construction grows unbounded is not quite complete. While $\frac{\partial\hat{\phi}_\alpha^{(0)}}{\partial\zeta_i}$ indeed vanishes in such a limit, $\hat{\phi}_\alpha^{(1)}(\zeta_i,\xi_i)$ and the domain of integration $\partial(i)$ grow arbitrarily large. The conclusion holds only when the rate of decay of the former is shown to be higher than the rate of growth of the latter two; otherwise, the argument is still nonrigorous. In the case of the local problem pertaining to binary interfaces, it can be rigorously shown that the leading-order term of the local asymptotic expansion converges to the matching requirement at an exponential rate [43]. Hence it may be a valuable assumption to invoke the same for the case of junctions, i.e., the solution of the p.d.e. system Eq. (10) as well. If so, the entire analysis of Sec. II A 2 will automatically be rigorously valid. Unfortunately, a proof of this exponential decay behavior is not currently available. Nevertheless, we turn our attention to the special case of triple junction to derive some insights. The explicit solution of the system of equations Eq. (10) is presented for the first time by Bollada *et al.* [53] when the chosen well is $W(\phi) = W^{\mathrm{FP}}(\phi) = a\{[\phi_1^2(1-\phi_1)^2 + \phi_2^2(1-\phi_2)^2 + \phi_3^2(1-\phi_3)^2]\}$, i.e., the one proposed by Folch and Plapp [37], and the junction is a triple point. Indeed it so happens that an

TABLE I. Table showing a parameter set used in the study of three phase growth within the setup of Fig. 6. N_x and N_y are the number of grid points in the x and y directions, respectively.

f_1	f_2	f_3	γ	τ_{12}	τ_{13}	N_x	N_y	Δx	Δt	ϵ
0.2	0.0	0.0	1.0	1.0	1.0	128	96	0.25	0.0125	$5.0 \times (\Delta x)^{0.6}$

$\{g_\alpha(\phi)\}$	$W(\phi)$	$\tau(\phi)$
$\{\phi_\alpha^3(10 - 15\phi_\alpha + 6\phi_\alpha^2)\}$	$W^{\mathrm{FP}} = 18[\phi_1^2(1-\phi_1)^2 + \phi_2^2(1-\phi_2)^2 + \phi_3^2(1-\phi_3)^2]$	$\frac{1}{\tau_{\mathrm{H}}(\phi)} = \frac{\sum_{\alpha<\beta} \frac{1}{\tau_{\alpha\beta}} \phi_\alpha^2 \phi_\beta^2}{\sum_{\alpha<\beta} \phi_\alpha^2 \phi_\beta^2}$

exponential decay is exhibited by $\frac{\partial \hat{\phi}_\alpha^{(0)}}{\partial \zeta_i}$ as ζ_i approaches ∞. Bollada *et al.*'s solution is studied in Appendix B where this tendency is explicitly demonstrated. We invoke an assumption that the exponential convergence behavior continues to remain true for any generic multiwell and a junction of any number of interfaces meeting. Then, the contribution from the integral of Eq. (23) to Eq. (22) is indeed zero. And similarly, the first integral on the r.h.s. of Eq. (25) will likewise identically vanish without any problem. In principle, in all the steps of going from Eq. (13) to Eq. (14), or from Eq. (15) to Eq. (16), or in establishing Eq. (26) or Eq. (27), an estimation of the relative rates of the convergence of the integrands and the divergence of the integration domains has to be performed to justify the deductions; which will all be taken care of, if the exponential decay assumption were to be invoked. In short, the analysis of Secs. II A 1 and II A 2 is complete if this assumption can be rigorously proven.

C. Mobilities' noninfluence on interfacial arrangement at junctions

Looking at Eqs. (17) and (18), it might be surprising to note that the mobilities of the interfaces have no say in how the latter arrange themselves at a junction. However, there is nothing really strange about how this result comes about. A comparison with the asymptotics routine for the binary interfaces will help expose the process. We consider the case of the standard (i.e., the scalar) Allen-Cahn equation:

$$\tau \frac{\partial \phi}{\partial t} = \frac{1}{\epsilon} \Delta f g'(\phi) - \gamma \frac{1}{\epsilon^2} f'_{\mathrm{dw}}(\phi) + \gamma \nabla^2 \phi. \tag{50}$$

At the leading order, the requirement of the local analysis of this equation is

$$\frac{\partial^2 \tilde{\phi}^{(0)}}{\partial \rho^2} = f'_{\mathrm{dw}}(\tilde{\phi}^{(0)}). \tag{51}$$

That is, it has only contributions coming from the gradient term and the well term. Only from the next order does the mobility start making an appearance in the emerging problem sequence characteristic of a perturbative method. Therefore, since the mobility does not show up in the leading-order problem, any information that can be extracted from the problem will be independent of it. For example, equipartition of the interfacial energy between the well term and the gradient term is a result that can be inferred from Eq. (51). Further, since τ does not appear in the equation, the result will remain unchanged no matter what admissible numerical value is chosen for it.

In the same manner, in the current case of junction analysis, at the leading order, the requirement is Eq. (10), and it is from this equation that the "force balance" requirements, Eqs. (17) and (18), are derived. Since the mobility function $\tau(\phi)$ does not contribute to this order, the result is independent of it; the independence on the bulk energies f_α is also for the same reason.

1. Numerical verification

We now present some numerical verification of this asymptotics predicted fact. Simulations in the same setup as in Fig. 6 are performed, but by assigning the ϕ_1 phase a higher bulk energy. As a result, there is a driving force for the phases on the bottom to grow at the expense of the one on the top. When it is high enough to overcome the curvature effects, the said growth indeed takes place, and eventually a steady state is attained. We carried out these simulations by numerically integrating Eq. (2) using an explicit finite difference scheme. The values of the inverse mobilities of the interfaces 1 and 2, i.e., τ_{12} and τ_{13}, are fixed at unity and that of τ_{23} is varied across three orders of magnitude. The exact parameter set used and the interpolation and multiwell forms employed for conducting the simulations are as given in Table I. The obtained steady-state growth fronts for various values of τ_{23} are displayed in Fig. 7 along with the sharp-interface predicted profile. It can be seen that the recovered results are practically independent of the mobility values. The computational steady-state speeds are tabulated in Table II and are compared with the sharp-interface analytical solution. Once again, the results remain practically the same for a change of τ_{23} across three orders of magnitude. Since all the three

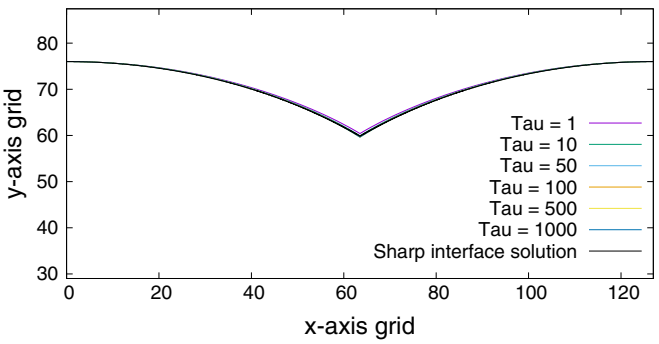

FIG. 7. Steady-state growth fronts realized in the simulations performed with the parameter set of Table I within the setup of Fig. 6 for various values of τ_{23}. Also depicted is the sharp-interface theory predicted profile in black.

TABLE II. Steady-state speeds recovered in the simulations corresponding to Fig. 7.

τ_{23}	Recovered angle at the triple junction	Recovered steady-state speed (rel. error)
1	30.86887°	0.071089274 (0.74%)
10	31.60365°	0.070363992 (1.75%)
50	31.76636°	0.070052259 (2.18%)
100	32.36498°	0.069987820 (2.27%)
500	32.22706°	0.069931031 (2.35%)
1000	32.27956°	0.069923091 (2.36%)
Sharp interface solution	30.0°	0.071616518

interfaces are chosen to have the same interfacial energy, the angle subtended by interface 1 with the x axis should be 30°. The simulation results, as is evident from column 2 of Table II, are in agreement with this, thus verifying the asymptotics prediction of noninfluence of interfacial mobilities in deciding the triple junction angles.

We note that the remaining errors found in Table II and their increasing trend down the columns is an artefact of the currently chosen interface width. Furthermore, the latter behavior, i.e., the deviation increasing as τ_{23} is made bigger, will become more drastic if an arithmetic form, viz. $\tau_{\mathrm{A}}(\phi) = \frac{\sum_{\alpha<\beta}\tau_{\alpha\beta}\phi_\alpha^2\phi_\beta^2}{\sum_{\alpha<\beta}\phi_\alpha^2\phi_\beta^2}$, were to be chosen for inverse mobility interpolation in place of the current $\tau_H(\phi)$ of Table I. The demonstration of this fact, the explanation for such a behavior, and the best prescription to carry out interface width reduction studies for its verification are too lengthy to fit into the current article, and hence are deferred to a follow-up one. We also point out that the validation through Fig. 7 and Table II is in no way an exhaustive numerical verification of the force balance requirement predicted by the asymptotics. The phases ϕ_2 and ϕ_3 are symmetric in the just presented numerical studies, whereas Eqs. (17) and (18) are valid for more general situations. In particular, we would like to vary the initial seed sizes of the two phases and then verify Eqs. (17) and (18). Folch and Plapp [37] gave steps for constructing an asymmetric triple well by means of which a system with all the three interfacial energies being different can be studied. Our current asymptotics is generic enough to apply for such a case. The mobilities τ_{12} and τ_{13} can also be taken to be different from one another and so can the bulk engeries f_2 and f_3. We would like to verify the validity of our force balance result for all such possible variations, although it must be admitted that it is going to be tricky to verify the Young's law in the latter two cases due to a very probable absence of steady-state modes. In the like manner, the comparison of the phase-field recovered steady-state velocities with the sharp interface solution in the third column of Table II is only an indirect verification of the equations of motion derived for junction kinetics, viz. Eqs (30) and (31). More direct proofs can be given by explicitly evaluating the integrals and the limits appearing in said equations either analytically or numerically. All these will be presented in a next article dedicated for the numerical verification of the asymptotics predicted junction dynamics.

V. CONCLUSION

An important question that can be asked about a multi-phase-field model is whether it recovers the Young's law for triple junctions at rest, and, what about when they are in motion? The most direct way of answering this is through asymptotic analysis which, unfortunately, is not usually performed at a level of rigour or completeness that is sufficient for this purpose. However, following Bronsard and Reitich [41], a full-fledged matching analysis is carried out for the problem of simple grain growth by the current authors over the span of two papers. The inner problem pertaining to the binary interfaces is analyzed in Ref. [43] while the junctions are given a thorough consideration in the current article. And the finding is that the angles subtended around a junction point by the meeting interfaces and their interfacial energies should always satisfy a force balance type condition whether or not it is in motion. For three interfaces, this translates to the validity of the Young's law for both the static and the dynamic situations.

The requirement of the force balance condition for junctions of any order (i.e., any number of meeting interfaces) immediately inspires a further query, namely that of stability. Particularly, it is well known from the experiments for soap bubbles and also those of grain-growth in pure metals that quadruple junctions are unstable over longer periods of time, and dissociate into two triple junctions. This naturally raises the question: While the asymptotic analysis infers which interfacial configurations are permissible around various junctions like triple, quadruple, etc., points, what explains the latter's relative stabilities?

Can it be Eq. (10)? That is, could it happen that the four phase version of Eq. (10) for a symmetric multiwell and for a quadruple point cannot have any solution that can give rise to a twofold rotationally symmetric interfacial arrangement thereby disallowing them a stable long term existence? On the other hand, not only the interfacial arrangement, but also the instantaneous speed of a junction point is determined by the asymptotic analysis and is as per Eqs. (30) and (31). So could it instead happen that twofold symmetric solutions well do exist for Eq. (10), and it is these kinetics laws, Eqs. (30) and (31), which actually determine the instability of the quadruple and higher order junctions? One of the focusses of our future investigations is going to be the pursuit of this inquiry further.

Most often, sharp-interface descriptions of three-phase evolutions are written down as though the whole of the governing physics pertaining to the junctions is completely exhausted by the Young's law. An additional equation dictating their instantaneous motion is typically not separately formulated and included. Since in our asymptotic analysis, apart from the Young's law, a condition governing the instantaneous velocity of the triple point is also recovered, it poses many new questions: Is this extra condition independent in its content, or is it derivable from the *Young's law + motion by mean curvature* combination [54]. In Ref. [41], short-time existence and uniqueness of evolution is indeed proved for this combination. Boundary integral solutions for a close by problem also suggest the same [55]. In such a case, an expression independent of fairly generic kinds of interpolation functions must be derivable from Eqs. (30) and (31). How to prove such

a strikingly surprising result? This is yet another interesting direction for research that emerged from the current work.

A crucial ingredient of the presented matching analysis that is only hypothesized but not proven is the assumption of exponential convergence of solutions of Eq. (10) to their "values at infinity." A stronger justification of this through a rigorous proof is very desirable.

While all these are very interesting topics for further investigation, they are more inclined to being problems in mainstream mathematics. A direction which is of immediate interest to the materials community is the asymptotic study of multiphase alloy evolution. That is, while the current study only looked at the phase-field evolution equation, it is of foremost interest to extend it by an inclusion of a chemical composition field.

Finally, for very similar models, a presence of definite influence of mobilities on the trijunction angles is observed in numerical simulations [38–40], whereas the current analysis predicts the opposite, which is also verified numerically in Sec. IV C. How can this contradiction be resolved? As it turns out, certain mobility interpolation functions impose severe demands on the interface thicknesses to have converged results for specific setups. Thus, by reducing the interface widths enough, the Young's law can be recovered even in the cases of the previously cited works. Demonstrations supporting this will be presented in an upcoming article.

ACKNOWLEDGMENTS

The authors gratefully acknowledge the funding by the German Research Foundation (DFG) through Grant No. NE822/31-1 (Gottfried-Wilhelm-Leibniz prize). The authors declare that they have no conflicts of interest.

APPENDIX A: DERIVATION OF MATCHING RELATIONS FOR JUNCTION REGIONS

Let a scalar field $\phi(x, y; \epsilon)$ have local asymptotic regular approximation along a path whose natural and stretched coordinates are (s, ρ). Let $s = 0$ correspond to the origin. Let the path correspond to the graph of a double differentiable function $f(x)$ with $f'(0) = 0$ for $s \in [0, 1]$. Let the asymptotic approximation be as follows:

$$\widetilde{\phi}(s, \rho; \epsilon) = \widetilde{\phi}^{(0)}(s, \rho) + \epsilon\widetilde{\phi}^{(1)}(s, \rho) + o(\epsilon) \quad \text{uniformly in} (s, \rho) \in [A, 1] \times [-B, B] \; \forall \, A > 0, B > 0.$$

By extension theorem, we have

$$\widetilde{\phi}(s, \rho; \epsilon) = \widetilde{\phi}^{(0)}(s, \rho) + \epsilon\widetilde{\phi}^{(1)}(s, \rho) + o(\epsilon) \quad \text{uniformly in } (s, \rho) \in [\epsilon^{\nu}, 1] \times \left[-\frac{1}{\epsilon^{\nu'}}, \frac{1}{\epsilon^{\nu'}}\right]. \tag{A1}$$

For the sake of convenience, we denote the interval $[\epsilon^{\nu}, 1]$ by R_s and $[-\frac{1}{\epsilon^{\nu'}}, \frac{1}{\epsilon^{\nu'}}]$ by R_ρ. For the reason expounded in Sec. III A, we take that $\nu' < 1$. The domain of validity when considered in the outer coordinates is

$$\begin{aligned} x(s, \rho) &= x_0(s) + \hat{n}_x(s)\rho\epsilon = x_0(s) - \frac{f'(x_0(s))}{\sqrt{1 + f'(x_0(s))^2}}\rho\epsilon \quad \forall (s, \rho) \in R_s \times R_\rho, \\ y(s, \rho) &= f(x_0(s)) + \hat{n}_y(s)\rho\epsilon = f(x_0(s)) + \frac{1}{\sqrt{1 + f'(x_0(s))^2}}\rho\epsilon \quad \forall (s, \rho) \in R_s \times R_\rho. \end{aligned} \tag{A2}$$

Since $\nu' < 1$, this means that for small enough ϵ, different (s, ρ) from the domain of validity corresponds to distinct spatial points. That is, there is no nonuniqueness in the representation of the points.

Next, let $\phi(x, y; \epsilon)$ exhibit a junction behavior at (0,0). In the junction's local coordinates $(\zeta = \frac{x}{\epsilon}, \xi = \frac{y}{\epsilon})$, let it have an asymptotic approximation as follows:

$$\hat{\phi}(\zeta, \xi; \epsilon) = \hat{\phi}^{(0)}(\zeta, \xi) + \epsilon\hat{\phi}^{(1)}(\zeta, \xi) + o(\epsilon) \quad \text{uniformly in } (\zeta, \xi) \in [0, C] \times [-D, D] \, \forall \, C > 0 \text{ and } D > 0. \tag{A3}$$

By extension theorem, we have

$$\hat{\phi}(\zeta, \xi; \epsilon) = \hat{\phi}^{(0)}(\zeta, \xi) + \epsilon\hat{\phi}^{(1)}(\zeta, \xi) + o(\epsilon) \quad \text{uniformly in} \quad (\zeta, \xi) \in [0, \epsilon^{-\mu}] \times \left[-\frac{1}{\epsilon^{\mu'}}, \frac{1}{\epsilon^{\mu'}}\right]. \tag{A4}$$

For a similar reason as in Sec. III A, let $\mu < 1$ and $\mu' < 1$.

We now re-express the domain of validity of the expansion of Eq. (A1) in terms of the (ζ, ξ) coordinate system. However, of interest is not an exact prescription but an estimation of the "end points" up to approximate powers of ϵ. Consider $x_0(s)$,

$$x_0(s) = x_0(0) + \left.\frac{dx_0}{ds}\right|_{s=0} s + \left.\frac{d^2x_0}{ds^2}\right|_{s=s_*} \frac{s^2}{2}. \tag{A5}$$

Since $x_0(s)$ is invertible and $x_0(0) = 0$, we have

$$\left.\frac{dx_0}{ds}\right|_{s=0} = \frac{1}{\left.\frac{ds}{dx_0}\right|_{x_0=0}} = \frac{1}{\sqrt{1 + f'(x_0(0))^2}} = \frac{1}{\sqrt{1 + f'(0)^2}} = 1, \tag{A6}$$

and

$$\left.\frac{d^2x_0}{ds^2}\right|_{s=s_*} = -\frac{f'(x_0(s_*))f''(x_0(s_*))}{\{1+f'(x_0(s_*))^2\}^2} = -\frac{f'(x_*)f''(x_*)}{(1+f'(x_*)^2)^2}, \tag{A7}$$

where $x_* = x_0(s_*) \leqslant s_*$. Since $f'(x_0(s))$ and $f''(x_0(s))$ are bounded $\forall\, s \in [0,1]$, this implies that when $s = \mathcal{O}_s(\epsilon^\nu)$, then $x_0(s) = \mathcal{O}_s(\epsilon^\nu)$. Therefore, for the domain of validity in Eq. (A1), $x_0(s) \in [A\epsilon^\nu, A']$ for some positive constants A and A'. Similarly, the upper and lower bounds for $\hat{n}_x(s)\rho\epsilon$ for the domain considered for (s,ρ) in Eq. (A1) can be estimated as

$$\begin{aligned}|\hat{n}_x(s)\rho\epsilon| &= \frac{\left|f'(x_0(0)) + f''(x_0(s))|_{s_*}\frac{dx_0}{ds}\big|_{s_*}s\right|}{\sqrt{1+f'(x_0(s))^2}}\rho\epsilon \\ &= \frac{|f''(x_0(s_*))|}{\sqrt{1+f'(x_0(s))^2}\sqrt{1+f'(x_0(s_*))^2}}s\rho\epsilon \in [\mathcal{O}_s(\epsilon^{\nu+1-\mu'}), \mathcal{O}_s(\epsilon^{1-\mu'})] \quad \text{when } (s,\rho)\in R_\nu. \end{aligned}\tag{A8}$$

Therefore, $x(s,\rho) \in [B\epsilon^\nu, B']$ for some positive B and B' which implies $\zeta \in [B\epsilon^{\nu-1}, B'\epsilon^{-1}]$ for the domain of the local approximation of Eq. (A1). We carry out similar analysis for $y(s,\rho)$:

$$\begin{aligned} y(s,\rho) &= f(0) + f'(0)x_0(s) + f''(x_*)\frac{x_0^2(s)}{2} + \frac{1}{\sqrt{1+f'(x_0(s))^2}}\rho\epsilon \\ &= f''(x_*)\frac{1}{2}\left(s + \left.\frac{d^2x_0}{ds^2}\right|_{s_{**}}\frac{s^2}{2}\right)^2 + \frac{1}{\sqrt{1+f'(x_0(s))^2}}\rho\epsilon \\ &= \mathcal{O}_s(\epsilon^{2\nu}) + \mathcal{O}_s(\epsilon^{1-\nu'}) \quad \text{when } s = \mathcal{O}_s(\epsilon^\nu) \quad \text{and } \rho = \mathcal{O}_s(1/\epsilon^{\nu'}). \end{aligned}\tag{A9}$$

Hence, $\xi \in [-C\epsilon^{-\max\{1-2\nu,\nu'\}}, C\epsilon^{-\max\{1-2\nu,\nu'\}}]$ for some $C > 0$ for the domain of the local approximation of Eq. (A1). As a consequence, Eq. (A1) can be re-expressed as follows:

$$\begin{aligned}\widetilde{\phi}(s(\epsilon\zeta,\epsilon\xi),\rho(\epsilon\zeta,\epsilon\xi);\epsilon) &= \widetilde{\phi}^{(0)}(s(\epsilon\zeta,\epsilon\xi),\rho(\epsilon\zeta,\epsilon\xi)) + \epsilon\widetilde{\phi}^{(1)}(s(\epsilon\zeta,\epsilon\xi),\rho(\epsilon\zeta,\epsilon\xi)) + o(\epsilon) \\ &\text{uniformly in } (\zeta,\xi) \in [B\epsilon^{\nu-1}, B'\epsilon^{-1}] \times [-C\epsilon^{-\max\{1-2\nu,\nu'\}}, C\epsilon^{-\max\{1-2\nu,\nu'\}}]. \end{aligned}\tag{A10}$$

We next proceed by assuming a strong overlap, i.e., $\epsilon^{\nu-1} < \epsilon^{-\mu}$. Furthermore, if $\lim_{\epsilon\to 0}\epsilon||\widetilde{\phi}^{(1)}(s,\rho)||_{L^\infty(R_s\times R_\rho)} = 0$ and $\lim_{\epsilon\to 0}\epsilon||\hat{\phi}^{(1)}(\zeta,\xi)||_{L^\infty([0,\epsilon^{-\mu}]\times[-1/\epsilon^{\mu'},1/\epsilon^{\mu'}])} = 0$, then

$$\begin{aligned}\widetilde{\phi}(s(\epsilon\zeta,\epsilon\xi),\rho(\epsilon\zeta,\epsilon\xi);\epsilon) &= \widetilde{\phi}^{(0)}(s(\epsilon\zeta,\epsilon\xi),\rho(\epsilon\zeta,\epsilon\xi)) + o(1) \quad \text{uniformly in} \\ &(\zeta,\xi) \in [B\epsilon^{\nu-1}, B'\epsilon^{-1}] \times [-C\epsilon^{-\max\{1-2\nu,\nu'\}}, C\epsilon^{-\max\{1-2\nu,\nu'\}}] \end{aligned}\tag{A11}$$

and

$$\hat{\phi}(\zeta,\xi) = \hat{\phi}^{(0)}(\zeta,\xi) + o(1) \text{ uniformly in } (\zeta,\xi) \in [0,\epsilon^{-\mu}] \times \left[-\frac{1}{\epsilon^{\mu'}}, \frac{1}{\epsilon^{\mu'}}\right]. \tag{A12}$$

We define $R_\zeta = [B\epsilon^{\nu-1}, \epsilon^{-\mu}]$ and $R_\xi = [-D\epsilon^{-\min\{\mu',\max\{1-2\nu,\nu'\}\}}, D\epsilon^{-\min\{\mu',\max\{1-2\nu,\nu'\}\}}]$ with $D = \min\{1, C\}$ in the following. Now consider

$$|\hat{\phi}^{(0)}(\zeta,\xi) - \widetilde{\phi}^{(0)}(s(\epsilon\zeta,\epsilon\xi),\rho(\epsilon\zeta,\epsilon\xi))| \text{ for any } (\zeta,\xi) \in R_\zeta \times R_\xi. \tag{A13}$$

One can write

$$\begin{aligned}|\hat{\phi}^{(0)}(\zeta,\xi) - \widetilde{\phi}^{(0)}(s(\epsilon\zeta,\epsilon\xi),\rho(\epsilon\zeta,\epsilon\xi))| &\leqslant |\hat{\phi}^{(0)}(\zeta,\xi) - \hat{\phi}(\zeta,\xi;\epsilon)| \\ &+ |\widetilde{\phi}^{(0)}(s(\epsilon\zeta,\epsilon\xi),\rho(\epsilon\zeta,\epsilon\xi)) - \widetilde{\phi}(s(\epsilon\zeta,\epsilon\xi),\rho(\epsilon\zeta,\epsilon\xi;\epsilon))| \\ &\leqslant \sup_{\zeta\in R_\zeta,\xi\in R_\xi}\{|\hat{\phi}^{(0)}(\zeta,\xi) - \hat{\phi}(\zeta,\xi;\epsilon) + |\widetilde{\phi}^{(0)}(s(\epsilon\zeta,\epsilon\xi),\rho(\epsilon\zeta,\epsilon\xi)) - \widetilde{\phi}(s(\epsilon\zeta,\epsilon\xi),\rho(\epsilon\zeta,\epsilon\xi;\epsilon))|\} \\ &\leqslant \sup_{\zeta\in[0,\epsilon^{-\mu}],\xi\in[-1/\epsilon^{\mu'},1/\epsilon^{\mu'}]}|\hat{\phi}^{(0)}(\zeta,\xi) - \hat{\phi}(\zeta,\xi;\epsilon)| \\ &+ \sup_{\substack{\zeta\in B\epsilon^{\nu-1},B'\epsilon^{-1}] \\ \xi\in[-C\epsilon^{-\max\{1-2\nu,\nu'\}},C\epsilon^{-\max\{1-2\nu,\nu'\}}]}}|\widetilde{\phi}^{(0)}(s(\epsilon\zeta,\epsilon\xi),\rho(\epsilon\zeta,\epsilon\xi)) - \widetilde{\phi}(s(\epsilon\zeta,\epsilon\xi),\rho(\epsilon\zeta,\epsilon\xi;\epsilon))|. \end{aligned}\tag{A14}$$

In the limit $\epsilon \to 0$, due to Eqs. (A11) and (A12), we have

$$\lim_{\epsilon\to 0}\{\hat{\phi}^{(0)}(\zeta,\xi) - \widetilde{\phi}^{(0)}(s(\epsilon\zeta,\epsilon\xi),\rho(\epsilon\zeta,\epsilon\xi))\} = 0 \text{ uniformly in } (\zeta,\xi) \in R_\zeta \times R_\xi \tag{A15}$$

or

$$\lim_{\epsilon\to 0}\hat{\phi}^{(0)}(\zeta,\xi)=\lim_{\epsilon\to 0}\widetilde{\phi}^{(0)}(s(\epsilon\zeta,\epsilon\xi),\rho(\epsilon\zeta,\epsilon\xi)) \tag{A16}$$

uniformly for all $(\zeta,\xi)\in R_\zeta\times R_\xi$, if the limits exist. Further, due to the domain of concern for (ζ,ξ) being the way it is, as $\epsilon\to 0$, ζ grows arbitrarily large. Let us now estimate the behavior of $s(\epsilon\zeta,\epsilon\xi)$ and $\rho(\epsilon\zeta,\epsilon\xi)$ as $\epsilon\to 0$, temporarily assuming that ζ and ξ are constants independent of ϵ, i.e., not in $R_\zeta\times R_\xi$. We rewrite them as

$$\begin{aligned}s(\epsilon\zeta,\epsilon\xi)&=s(0,\epsilon\xi)+\left.\frac{\partial s}{\partial x}\right|_{(\epsilon\zeta_*,\epsilon\xi)}\epsilon\zeta\\&=s(0,\epsilon\xi)+\left.\frac{ds}{dx_0}\right|_{x_0(\epsilon\zeta_*,\epsilon\xi)}\left.\frac{\partial x_0}{\partial x}\right|_{(\epsilon\zeta_*,\epsilon\xi)}\epsilon\zeta=0+\sqrt{1+f'(x_0(\epsilon\zeta_*,\epsilon\xi))^2}\left.\frac{\partial x_0}{\partial x}\right|_{(\epsilon\zeta_*,\epsilon\xi)}\epsilon\zeta\end{aligned} \tag{A17}$$

and

$$\rho(\epsilon\zeta,\epsilon\xi)=\rho(0,\epsilon\xi)+\left.\frac{\partial\rho}{\partial x}\right|_{(0,\epsilon\xi)}\epsilon\zeta+\left.\frac{\partial^2\rho}{\partial x^2}\right|_{(\epsilon\zeta_*,\epsilon\xi)}\frac{\epsilon^2\zeta^2}{2}=\xi+\left.\frac{\partial r}{\partial x}\right|_{(0,\epsilon\xi)}\zeta+\left.\frac{\partial^2 r}{\partial x^2}\right|_{(\epsilon\zeta_*,\epsilon\xi)}\frac{\epsilon\zeta^2}{2}, \tag{A18}$$

where $x_0(\epsilon\zeta,\epsilon\xi)$ is the solution of Eq. (44) and $r(x,y)$ is given by Eq. (41). Since it is established that each $(\epsilon\zeta,\epsilon\xi)$ for the domain concerned for (ζ,ξ) has a unique representation in the (s,ρ) coordinate system for small enough ϵ, $x_0(\epsilon\zeta_*,\epsilon\xi)\to 0$ as $\epsilon\to 0$. Further, differentiating Eq. (42), we have

$$\begin{aligned}&\frac{\partial x_0}{\partial x}-yf''(x_0)\frac{\partial x_0}{\partial x}+f'(x_0)^2\frac{\partial x_0}{\partial x}+f(x_0)f''(x_0)\frac{\partial x_0}{\partial x}=1\\&\Rightarrow\left.\frac{\partial x_0}{\partial x}\right|_{(\epsilon\zeta_*,\epsilon\xi)}=\frac{1}{(1-\epsilon\xi f''(x_0)+(f'(x_0))^2+f(x_0)f''(x_0))}\Rightarrow\left.\frac{\partial x_0}{\partial x}\right|_{(\epsilon\zeta_*,\epsilon\xi)}\to 1\ \text{as}\ \epsilon\to 0.\end{aligned} \tag{A19}$$

Similarly, from Eq. (41), for $\frac{\partial r}{\partial x}$ we have

$$\left.\frac{\partial r}{\partial x}\right|_{(x,y)}=\frac{x-x_0}{\sqrt{(x-x_0)^2+(y-f(x_0))^2}}\Rightarrow\left.\frac{\partial r}{\partial x}\right|_{(0,\epsilon\xi)}=0. \tag{A20}$$

For $\frac{\partial^2 r}{\partial x^2}$, we have

$$\left.\frac{\partial^2 r}{\partial x^2}\right|_{(x,y)}=-\frac{r\left(1-\frac{\partial x_0}{\partial x}\right)-(x-x_0)\frac{\partial r}{\partial x}}{r^2}=-\kappa(x_0)\frac{1}{\{1-yf''(x_0)+(f'(x_0))^2+f(x_0)f''(x_0)\}}, \tag{A21}$$

where $\kappa(x_0)$ is the curvature of the function $f(x)$ at x_0 and is defined as $\kappa(x)=\frac{f''(x)}{\{\sqrt{1+[f'(x)]^2}\}^3}$. That is, with the convention that concave upwards is positively curved. The upshot being

$$\left.\frac{\partial^2 r}{\partial x^2}\right|_{(\epsilon\zeta_*,\epsilon\xi)}\to-\kappa(0)\ \text{as}\ \epsilon\to 0. \tag{A22}$$

Equations (A17), (A18), (A19), (A20), (A22), and the associated analysis indicate that $s(\epsilon\zeta,\epsilon\xi)\to 0$ and $\rho(\epsilon\zeta,\epsilon\xi)\to\xi$ as $\epsilon\to 0$ for $(\zeta,\xi)\in R_\zeta\times R_\xi$ as well. Which implies that Eq. (A16) modifies as

$$\boxed{\lim_{\zeta\to\infty}\hat{\phi}^{(0)}(\zeta,\xi)=\lim_{s\to 0}\widetilde{\phi}^{(0)}(s,\xi)} \tag{A23}$$

This is the matching relation for the zeroth order term of the local expansion corresponding to the junction point. We repeat the above analysis from Eq. (A13) but for Eqs. (A4) and (A10) to obtain the matching condition for the first-order correction:

Consider

$$\left|\hat{\phi}^{(1)}(\zeta,\xi)+\frac{1}{\epsilon}\hat{\phi}^{(0)}(\zeta,\xi)-\widetilde{\phi}^{(1)}(s(\epsilon\zeta,\epsilon\xi))-\frac{1}{\epsilon}\widetilde{\phi}^{(0)}(s(\epsilon\zeta,\epsilon\xi))\right| \quad \text{for any } (\zeta,\xi)\in R_\zeta\times R_\xi \tag{A24}$$

$$\Rightarrow \lim_{\epsilon\to 0}\left\{\hat{\phi}^{(1)}(\zeta,\xi)-\widetilde{\phi}^{(1)}(s(\epsilon\zeta,\epsilon\xi),\rho(\epsilon\zeta,\epsilon\xi))\right.$$
$$\left.-\frac{1}{\epsilon}\left[\widetilde{\phi}^{(0)}\left(0+\left.\frac{\partial s}{\partial x}\right|_{(\epsilon\zeta_*,\epsilon\xi)}\epsilon\zeta,\xi+0+\left.\frac{\partial^2 r}{\partial x^2}\right|_{(\epsilon\zeta_*,\epsilon\xi)}\frac{\epsilon\zeta^2}{2}\right)-\hat{\phi}^{(0)}(\zeta,\xi)\right]\right\}=0$$
uniformly for $(\zeta,\xi)\in R_\zeta\times R_\xi$

$$\Rightarrow \lim_{\zeta\to\infty}\lim_{\epsilon\zeta\to 0}\lim_{\epsilon\to 0}\left\{\hat{\phi}^{(1)}(\zeta,\xi)-\widetilde{\phi}^{(1)}(s(\epsilon\zeta,\epsilon\xi),\rho(\epsilon\zeta,\epsilon\xi))\right.$$
$$\left.-\frac{1}{\epsilon}\left[\widetilde{\phi}^{(0)}(0,\xi)+\left.\frac{\partial\widetilde{\phi}^{(0)}}{\partial s}\right|_{(*,*)}\left.\frac{\partial s}{\partial x}\right|_{(\epsilon\zeta_*,\epsilon\xi)}\epsilon\zeta+\left.\frac{\partial\widetilde{\phi}^{(0)}}{\partial\rho}\right|_{(*,*)}\left.\frac{\partial^2 r}{\partial x^2}\right|_{(\epsilon\zeta_*,\epsilon\xi)}\frac{\epsilon\zeta^2}{2}-\hat{\phi}^{(0)}(\zeta,\xi)\right]\right\}=0$$
for all $\xi\in\mathbb{R}$

$$\Rightarrow \boxed{\hat{\phi}^{(1)}(\zeta,\xi)=\lim_{s\to 0}\left(\widetilde{\phi}^{(1)}(s,\xi)+\zeta\frac{\partial\widetilde{\phi}^{(0)}}{\partial s}(s,\xi)-\frac{\kappa(0)}{2}\zeta^2\frac{\partial\widetilde{\phi}^{(0)}}{\partial\rho}(s,\xi)\right)+o(1)\text{ as }\zeta\to\infty} \tag{A25}$$

assuming that the limit exists and that $\lim_{\epsilon\to 0}\hat{\phi}^{(0)}(\epsilon^{-\mu},\xi)$ approaches $\widetilde{\phi}^{(0)}(0,\xi)$ faster than ϵ as well as that the other errors remain vanishingly small.

Although the above derivation is presented for the case of a scalar field $\phi(x,y;\epsilon)$, the same arguments work for the vector case as well, as uniform continuity of a vector valued function implies and is implied by the like behavior of its components. Further, when viewed from the coordinate system (ζ_i,ξ_i), the ith interface up to some arc length will necessarily look like the trace of a function, i.e., can be expressible as $(\zeta_i, f(\zeta_i))$ for some nonzero interval of ζ_i. Further, due to the way in which these coordinates are selected, $f'(\zeta_i)$ necessarily vanishes at $\zeta_i=0$. Also, it is easy to see that the right end-point of s in Eq. (A1) being at unity can be easily disposed off. Thus, from Eqs. (A23) and (A25), Eqs. (8) and (9) readily follow. Furthermore, nowhere in the above derivation, the boundary layer or the interior layer behavior along the path of $r=0$ was crucial for the analysis. A mere existence of an asymptotic expansion is all that suffices. But this is true even if no singular behavior exists at the path of the function $f(x)$. Thus, if a path were to be chosen completely inside any of the "bulks," then the derivation still applies with the only change being that all $\widetilde{\phi}^{(q)}(s,\rho)$, $q\geqslant 1$ in Eq. (A1) and thus in Eq. (9) are identically zeros. Further, $\widetilde{\phi}^{(0)}(s,\rho)$ will be a constant, and hence, the r.h.s. of Eq. (9) as a whole vanishes. This justifies our treatment for the "open-side" of the polygonal construction in Sec. II A 1, as the path chosen there is a straight line completely lying inside a bulk.

APPENDIX B: ANALYSIS OF THE EXPLICIT SOLUTION OF EQ. (10) FOR W^{FP} MULTIWELL

The system of equations of Eq. (10) written down explicitly for the multiwell W^{FP} read

$$\begin{aligned}
\frac{\partial^2\hat{\phi}_1^{(0)}}{\partial\zeta^2}+\frac{\partial^2\hat{\phi}_1^{(0)}}{\partial\xi^2}&=4a\hat{\phi}_1^{(0)}\left(\hat{\phi}_1^{(0)}-0.5\right)\left(\hat{\phi}_1^{(0)}-1\right)-\frac{4a}{3}\sum_{\alpha=1}^{3}\hat{\phi}_\alpha^{(0)}\left(\hat{\phi}_\alpha^{(0)}-0.5\right)\left(\hat{\phi}_\alpha^{(0)}-1\right),\\
\frac{\partial^2\hat{\phi}_2^{(0)}}{\partial\zeta^2}+\frac{\partial^2\hat{\phi}_2^{(0)}}{\partial\xi^2}&=4a\hat{\phi}_2^{(0)}\left(\hat{\phi}_2^{(0)}-0.5\right)\left(\hat{\phi}_2^{(0)}-1\right)-\frac{4a}{3}\sum_{\alpha=1}^{3}\hat{\phi}_\alpha^{(0)}\left(\hat{\phi}_\alpha^{(0)}-0.5\right)\left(\hat{\phi}_\alpha^{(0)}-1\right),\\
\frac{\partial^2\hat{\phi}_3^{(0)}}{\partial\zeta^2}+\frac{\partial^2\hat{\phi}_3^{(0)}}{\partial\xi^2}&=4a\hat{\phi}_3^{(0)}\left(\hat{\phi}_3^{(0)}-0.5\right)\left(\hat{\phi}_3^{(0)}-1\right)-\frac{4a}{3}\sum_{\alpha=1}^{3}\hat{\phi}_\alpha^{(0)}\left(\hat{\phi}_\alpha^{(0)}-0.5\right)\left(\hat{\phi}_\alpha^{(0)}-1\right),
\end{aligned} \tag{B1}$$

when it is kept in mind that the solution space is restricted to functions satisfying the summation rule property, i.e., $\hat{\phi}_1^{(0)}(\zeta,\xi)+\hat{\phi}_2^{(0)}(\zeta,\xi)+\hat{\phi}_3^{(0)}(\zeta,\xi)=1\ \forall\ (\zeta,\xi)\in\mathbb{R}^2$.

Bollada *et al.* [53] proposed a possible multi-phase-field profile around a triple junction by generalizing the "tanh solution" of the 1D problem. Using it, they studied what gradient energy will be associated with a spatial point corresponding to a particular phase field value, for various choices of the gradient energy forms. However, it is unclear from the article if it is indeed explicitly verified whether the proposed profile does actually solve the equilibrium equations for any of the combinations of the potential wells and the gradient energy forms considered. It will now be tested if the postulated profile, which is reproduced in Eq. (B2), is the solution of Eq. (B1).

1. Verification of the exactness

The equilibrium phase-field profile around a triple junction hypothesized by Bollada *et al.* is considered as a potential candidate for the solution of Eq. (B1). That is,

$$\hat{\phi}_1^{(0)} = \frac{1}{1 + e^{(\zeta n_{12}^{\zeta} + \xi n_{12}^{\xi})} + e^{(\zeta n_{13}^{\zeta} + \xi n_{13}^{\xi})}}, \quad \hat{\phi}_2^{(0)} = \frac{1}{1 + e^{(\zeta n_{21}^{\zeta} + \xi n_{21}^{\xi})} + e^{(\zeta n_{23}^{\zeta} + \xi n_{23}^{\xi})}}, \quad \hat{\phi}_3^{(0)} = \frac{1}{1 + e^{(\zeta n_{31}^{\zeta} + \xi n_{31}^{\xi})} + e^{(\zeta n_{32}^{\zeta} + \xi n_{32}^{\xi})}}, \tag{B2}$$

where n_{ij}^{ζ} and n_{ij}^{ξ} are the ζ and ξ components of a vector $\mathbf{n_{ij}}$ which is (i) normal to the interface between phases ϕ_i and ϕ_j, (ii) at the triple junction, and (iii) pointing toward phase ϕ_j (and hence away from phase ϕ_i). Further, the vectors $\mathbf{n_{ij}}$ should satisfy $\mathbf{n_{12}} + \mathbf{n_{23}} + \mathbf{n_{31}} = 0$. This makes sure that the component functions $\hat{\phi}_{\alpha}^{(0)}$ satisfy the summation rule which can be quickly shown by re-expressing Eq. (B2) in the following manner by using it:

$$\begin{aligned}
\hat{\phi}_1^{(0)} &= \frac{1}{1 + e^{(\zeta n_{12}^{\zeta} + \xi n_{12}^{\xi})} + e^{(\zeta n_{13}^{\zeta} + \xi n_{13}^{\xi})}}, \quad \hat{\phi}_2^{(0)} = \frac{1}{1 + e^{-(\zeta n_{12}^{\zeta} + \xi n_{12}^{\xi})} + e^{(\zeta n_{23}^{\zeta} + \xi n_{23}^{\xi})}} = \frac{e^{(\zeta n_{12}^{\zeta} + \xi n_{12}^{\xi})}}{1 + e^{(\zeta n_{12}^{\zeta} + \xi n_{12}^{\xi})} + e^{(\zeta n_{13}^{\zeta} + \xi n_{13}^{\xi})}}, \\
\hat{\phi}_2^{(0)} &= \frac{1}{1 + e^{-(\zeta n_{13}^{\zeta} + \xi n_{13}^{\xi})} + e^{(\zeta n_{32}^{\zeta} + \xi n_{32}^{\xi})}} = \frac{e^{(\zeta n_{13}^{\zeta} + \xi n_{13}^{\xi})}}{1 + e^{(\zeta n_{12}^{\zeta} + \xi n_{12}^{\xi})} + e^{(\zeta n_{13}^{\zeta} + \xi n_{13}^{\xi})}}.
\end{aligned} \tag{B3}$$

Expressed in this form, the summation property is easy to verify.

Substituting Eq. (B3) in Eq. (B1), and verifying if the latter is satisfied for some constant "a" could be a very cumbersome and lengthy calculation. To minimize this, we make the following observations. First, due to the nature of the equations in Eq. (B1), if $(\hat{\phi}_1^{(0)}, \hat{\phi}_2^{(0)}, \hat{\phi}_3^{(0)})$ is a solution, then a rotation of it about the origin is also a solution. Thus, without loss of generality, one of the interfaces can be oriented along the ζ axis. Specifically, we choose the phase above the positive axis as ϕ_1, therefore, $\mathbf{n_{12}}$ is $-\hat{\xi}$. Second, Eq. (B3) may or may not solve Eq. (B1) for any given three vectors $\mathbf{n_{12}}$, $\mathbf{n_{23}}$, and $\mathbf{n_{31}}$ satisfying $\mathbf{n_{12}} + \mathbf{n_{23}} + \mathbf{n_{31}} = 0$. However, we are only interested in vectors that are 120-120-120 degrees apart, as that is what the demand of the asymptotic analysis is in the present problem of interest (equal interfacial energies). Hence, it will be enough to test the case of $\mathbf{n_{12}}$, $\mathbf{n_{23}}$, and $\mathbf{n_{23}}$ being unit vectors. In fact, this is exactly the recommendation of Bollada *et al.* when the interfacial energies are all equal. Thus, as $\mathbf{n_{12}}$ is fixed as $-\hat{\xi}$, $\mathbf{n_{23}}$ and $\mathbf{n_{23}}$ readily get determined and the test solution becomes

$$\hat{\phi}_1^{(0)} = \frac{1}{1 + e^{-\xi} + e^{-\frac{\sqrt{3}}{2}\zeta - \frac{1}{2}\xi}}, \quad \hat{\phi}_2^{(0)} = \frac{e^{-\xi}}{1 + e^{-\xi} + e^{-\frac{\sqrt{3}}{2}\zeta - \frac{1}{2}\xi}}, \quad \hat{\phi}_3^{(0)} = \frac{e^{-\frac{\sqrt{3}}{2}\zeta - \frac{1}{2}\xi}}{1 + e^{-\xi} + e^{-\frac{\sqrt{3}}{2}\zeta - \frac{1}{2}\xi}}. \tag{B4}$$

Note that the r.h.s. of the last equation of Eq. (B1) is the same as the sum of the r.h.s. of the first two equations but with a negative sign irrespective of what $\hat{\phi}_1^{(0)}$, $\hat{\phi}_2^{(0)}$, and $\hat{\phi}_3^{(0)}$ are. Further, when these latter are chosen to satisfy the summation rule, the left-hand sides of Eq. (B1), as well, behave identically, i.e., add up to zero. Therefore, it follows that it suffices to check the validity of only the first two equations. These latter can be rewritten further as follows to facilitate a reduction of number of algebra steps:

$$\begin{aligned}
\frac{\partial^2 \hat{\phi}_1^{(0)}}{\partial \zeta^2} + \frac{\partial^2 \hat{\phi}_1^{(0)}}{\partial \xi^2} &= 4a\hat{\phi}_1^{(0)}\left(\hat{\phi}_1^{(0)} - 0.5\right)\left(\hat{\phi}_1^{(0)} - 1\right) - 4a\hat{\phi}_1^{(0)}\hat{\phi}_2^{(0)}\hat{\phi}_3^{(0)}, \\
\frac{\partial^2 \hat{\phi}_2^{(0)}}{\partial \zeta^2} + \frac{\partial^2 \hat{\phi}_2^{(0)}}{\partial \xi^2} &= 4a\hat{\phi}_2^{(0)}\left(\hat{\phi}_2^{(0)} - 0.5\right)\left(\hat{\phi}_2^{(0)} - 1\right) - 4a\hat{\phi}_1^{(0)}\hat{\phi}_2^{(0)}\hat{\phi}_3^{(0)}.
\end{aligned}$$

Substituting Eq. (B4) in the above equations shows that the latter are satisfied for $a = 0.5$. Thus, Eq. (B2) with unit vectors $\mathbf{n_{12}}$, $\mathbf{n_{23}}$, and $\mathbf{n_{31}}$ satisfying $\mathbf{n_{12}} + \mathbf{n_{23}} + \mathbf{n_{31}} = 0$ is the exact solution of the leading-order junction equations for the Folch-Plapp multiwell with $a = 0.5$.

2. Exponential "decay"

It will now be shown that approaching infinity along lines parallel to the interfacial directions recovers the consequent limiting values of $(\hat{\phi}_1^{(0)}, \hat{\phi}_2^{(0)}, \hat{\phi}_3^{(0)})$ at an exponential rate. First, let us consider the particular case of Eq. (B4), i.e., when one of the interfaces is along the positive ζ axis. Now, let us approach infinity always staying at a distance of δ from the latter. That is, we travel along the ray $\overrightarrow{r}(\rho) = (0, \delta) + \rho \times (1, 0)$ as $\rho \to \infty$. The result is

$$\lim_{\rho \to \infty} \hat{\phi}^{(0)}(\rho, \delta) = \left(\frac{1}{1 + e^{-\delta} + 0}, \frac{e^{-\delta}}{1 + e^{-\delta} + 0}, \frac{0}{1 + e^{-\delta} + 0}\right) = \left(\frac{1}{1 + e^{-\delta}}, \frac{e^{-\delta}}{1 + e^{-\delta}}, 0\right).$$

To find the rate at which this "value" is converged to, we subtract $\hat{\phi}^{(0)}(\rho, \delta)$ from the limiting value. Particularly, considering the first component, we have

$$\frac{1}{1 + e^{-\delta}} - \hat{\phi}_1^{(0)}(\rho, \delta) = \left|\frac{1}{1 + e^{-\delta}} - \hat{\phi}_1^{(0)}(\rho, \delta)\right| = \frac{e^{-\frac{\sqrt{3}}{2}\rho - \frac{1}{2}\delta}}{(1 + e^{-\delta})(1 + e^{-\delta} + e^{-\frac{\sqrt{3}}{2}\rho - \frac{1}{2}\delta})} < e^{-\frac{\sqrt{3}}{2}\rho - \frac{1}{2}\delta}.$$

That is, the first component exponentially attains its limiting value as $\rho \to \infty$; similar calculations reveal the same for the others as well.

The above is for that interface lying along ζ axis, the like nature of the others can be argued without reperforming the calculations: Rotating the solution $\hat{\phi}_1^{(0)}(\zeta, \xi)$ by 120° and 270°, the other interfaces will align along the ζ axis. Furthermore, the resultant components will be permutations of the current ones. Since, the functional forms remain unchanged, the convergence behavior carries over.

[1] L.-Q. Chen, Annu. Rev. Mater. Res. **32**, 113 (2002).
[2] L.-Q. Chen and Y. Zhao, Prog. Mater. Sci. **124**, 100868 (2022).
[3] L.-Q. Chen, J. Am. Ceram. Soc. **91**, 1835 (2008).
[4] N. Moelans, B. Blanpain, and P. Wollants, Calphad **32**, 268 (2008).
[5] I. Bellemans, N. Moelans, and K. Verbeken, Crit. Rev. Solid State Mater. Sci. **43**, 417 (2018).
[6] I. Steinbach and O. Shchyglo, Curr. Opin. Solid State Mater. Sci. **15**, 87 (2011).
[7] I. Steinbach, JOM **65**, 1096 (2013).
[8] I. Steinbach, Modell. Simul. Mater. Sci. Eng. **17**, 073001 (2009).
[9] I. Steinbach, Annu. Rev. Mater. Res. **43**, 89 (2013).
[10] W. J. Boettinger, J. A. Warren, C. Beckermann, and A. Karma, Annu. Rev. Mater. Res. **32**, 163 (2002).
[11] L. Gránásy, G. I. Tóth, J. A. Warren, F. Podmaniczky, G. Tegze, L. Rátkai, and T. Pusztai, Prog. Mater. Sci. **106**, 100569 (2019).
[12] H. Chan, M. Cherukara, T. D. Loeffler, B. Narayanan, and S. K. R. S. Sankaranarayanan, npj Comput. Mater. **6**, 1 (2020).
[13] H. Emmerich, Adv. Phys. **57**, 1 (2008).
[14] A. C. Powell, Y. Shibuta, J. E. Guyer, and C. A. Becker, JOM **59**, 35 (2007).
[15] M. Ode, S. G. Kim, and T. Suzuki, ISIJ Int. **41**, 1076 (2001).
[16] B. Nestler and A. Choudhury, Curr. Opin. Solid State Mater. Sci. **15**, 93 (2011).
[17] D. Tourret, H. Liu, and J. LLorca, Prog. Mater. Sci. **123**, 100810 (2022).
[18] B. Saswata, B. Soumya, and C. Abhik, J. Indian Inst. Sci. **96**, 257 (2016).
[19] K. Michael, S. Philipp, N. Britta *et al.*, J. Indian Inst. Sci. **96**, 235 (2016).
[20] P. Mathis, J. Indian Inst. Sci. **96**, 179 (2016).
[21] N. Provatas, T. Pinomaa, and N. Ofori-Opoku, *Quantitative Phase Field Modelling of Solidification* (CRC Press, Boca Raton, FL, 2021).
[22] J. W. Cahn, Acta Metall. **9**, 795 (1961).
[23] J. W. Cahn, Acta Metall. **10**, 179 (1962).
[24] R. Kobayashi, Physica D **63**, 410 (1993).
[25] A. A. Wheeler, W. J. Boettinger, and G. B. McFadden, Phys. Rev. A **45**, 7424 (1992).
[26] J. A. Warren and W. J. Boettinger, Acta Metall. Mater. **43**, 689 (1995).
[27] J. A. Warren and B. T. Murray, Modell. Simul. Mater. Sci. Eng. **4**, 215 (1996).
[28] M. Ode, T. Suzuki, S. G. Kim, and W. T. Kim, Mater. Trans. **42**, 2410 (2001).
[29] G. Caginalp, Arch. Ration. Mech. Anal. **92**, 205 (1986).
[30] G. Caginalp, Phys. Rev. A **39**, 5887 (1989).
[31] R. F. Almgren, SIAM J. Appl. Math. **59**, 2086 (1999).
[32] J. W. Cahn, C. M. Elliott, and A. Novick-Cohen, Eur. J. Appl. Math **7**, 287 (1996).
[33] P. W. Hoffrogge, A. Mukherjee, E. S. Nani, P. G. Kubendran Amos, F. Wang, D. Schneider, and B. Nestler, Phys. Rev. E **103**, 033307 (2021).
[34] A. Karma and W.-J. Rappel, Phys. Rev. E **57**, 4323 (1998).
[35] T. Young, in *Abstracts of the Papers Printed in the Philosophical Transactions of the Royal Society of London*, Vol. 1 (The Royal Society London, 1832), pp. 171–172.
[36] F. Boyer and C. Lapuerta, ESAIM: Math. Modell. Numer. Anal. **40**, 653 (2006).
[37] R. Folch and M. Plapp, Phys. Rev. E **72**, 011602 (2005).
[38] S. Ghosh, A. Karma, M. Plapp, S. Akamatsu, S. Bottin-Rousseau, and G. Faivre, Acta Mater. **175**, 214 (2019).
[39] F. Wendler, A. Okamoto, and P. Blum, Geofluids **16**, 211 (2016).
[40] N. Prajapati, A. Abad Gonzalez, M. Selzer, B. Nestler, B. Busch, and C. Hilgers, J. Geophys. Res.: Solid Earth **125**, e2019JB019137 (2020).
[41] L. Bronsard and F. Reitich, Arch. Ration. Mech. Anal. **124**, 355 (1993).
[42] A. A. Wheeler, G. McFadden, and W. Boettinger, Proc. Roy. Soc. London. Series A: Math., Phys. Eng. Sci. **452**, 495 (1996).
[43] E. S. Nani and B. Nestler, Phys. Rev. E **105**, 014802 (2022).
[44] Otherwise, depending on which phase it is viewed in relation to, the same value would correspond to both a stable phase and an intermediate one, and hence has to be sustained and penalized at the same time, which is a contradiction.
[45] D. Fan and L.-Q. Chen, Acta Mater. **45**, 611 (1997).
[46] C. E. Krill III and L.-Q. Chen, Acta Mater. **50**, 3059 (2002).
[47] S. G. Kim, D. I. Kim, W. T. Kim, and Y. B. Park, Phys. Rev. E **74**, 061605 (2006).
[48] N. Moelans, F. Wendler, and B. Nestler, Comput. Mater. Sci. **46**, 479 (2009).
[49] I. McKenna, S. Poulsen, E. M. Lauridsen, W. Ludwig, and P. W. Voorhees, Acta Mater. **78**, 125 (2014).
[50] R. Perumal, P. K. Amos, M. Selzer, and B. Nestler, Comput. Mater. Sci. **140**, 209 (2017).
[51] R. Perumal, P. K. Amos, M. Selzer, and B. Nestler, Comput. Mater. Sci. **147**, 227 (2018).
[52] W. Eckhaus, *Asymptotic Analysis of Singular Perturbations* (Elsevier, Amsterdam, 2011).
[53] P. Bollada, P. Jimack, and A. Mullis, Comput. Mater. Sci. **171**, 109085 (2020).
[54] The motion by mean curvature is recovered as the limiting case behavior for the binary interfaces for the current model in the precursory paper to the current one, Ref. [43].
[55] A. Karma and A. Sarkissian, Metal. Mater. Trans. A **27**, 635 (1996).